Research Square

Preprints are preliminary reports that have not undergone peer review.
They should not be considered conclusive, used to inform clinical practice,
or referenced by the media as validated information.

The regulatory effect of root exudates from medicinal plants on rhizosphere microbial community structure under understory cultivation mode

Yuan YANG
College of Agriculture and Biotechnology, Yunnan Agricultural University
Jianqiang LI
JQ-Lee83125@hotmail.com
School of Soil and Water Conservation, Southwest Forestry University
Bo YANG
School of Soil and Water Conservation, Southwest Forestry University
Wen CHEN
School of Soil and Water Conservation, Southwest Forestry University
Wenqi TANG
School of Soil and Water Conservation, Southwest Forestry University
Lianling CHA
School of Soil and Water Conservation, Southwest Forestry University

Research Article

Keywords: Under-forest Panax notoginseng, Under-forest Polygonatum sibiricum, Under-forest Eutrema wasabia, Root exudates, Soil nutrients, Soil rhizosphere microorganisms

Posted Date: October 22nd, 2026

DOI: https://doi.org/10.21203/rs.3.rs-11186519/v1

License: This work is licensed under a Creative Commons Attribution 4.0 International License.
Read Full License

Additional Declarations: No competing interests reported.

The regulatory effect of root exudates from medicinal plants on rhizosphere microbial community structure under understory cultivation mode

Yuan YANG[1], Jianqiang LI[2]*, Bo YANG[2], Wen CHEN[2], Wenqi TANG[2], Lianling CHA[2]
1.Yunnan Agricultural University , Kunming, Yunnan Province, 650500, China

2.Southwest Forestry University , Kunming, Yunnan Province, 650224, China

Jianqiang Li（corresponding author）email:JQ-Lee83125@hotmail.com

Abstract: Understory cultivation of medicinal plants is a promising ecological forestry model, yet the mechanisms by which root exudates mediate rhizosphere microbial assemblages and plant quality formation remain unclear. In this study, we investigated the chemical characteristics of root exudates, rhizosphere microbial community composition, and metabolic pathway enrichment of three medicinal plants ***Panax notoginseng*** (DPN), ***Polygonatum sibiricum*** (DPS), and ***Eutrema wasabia*** (DEW) cultivated under a natural forest, using untargeted metabolomics and amplicon sequencing.Root exudates exhibited pronounced species specificity: compared with the non-planted control (DCK), the three species secreted 355, 236, and 241 significantly different metabolites, respectively, with 89 shared differential metabolites. Lipids and lipid-like molecules dominated in all species, followed by organic acids and derivatives, organic oxygen compounds, and phenylpropanoids and polyketides. Exudate inputs significantly shaped the structure, abundance, and diversity of dominant bacterial phyla (***Pseudomonadota, Acidobacteriota, Chloroflexita, Actinomycota***) and fungal phyla (***Ascomycota, Basidiomycota, Mortierellomycota***). Procrustes analysis and the Mantel test ($r>0.4$, $P<0.001$) confirmed significant coupling between exudate metabolites and microbial community structure, with fungi showing tighter chemical–biological linkage, indicating a positive recruitment effect of root exudates on rhizosphere microorganisms.KEGG enrichment revealed differential adaptation strategies: ***Panax notoginseng*** enriched 71 pathways (23 significant), centering on plant hormone signal transduction, aminoacyl-tRNA biosynthesis, and the TCA cycle; ***Polygonatum sibiricum*** enriched 52 pathways (16 significant), highlighting nucleotide metabolism and ABC transporters; ***Eutrema wasabia*** enriched 44 pathways (8 significant), characterized by linoleic acid metabolism and flavonoid biosynthesis. Microbial–metabolite network analysis further demonstrated treatment-specific associations: ***Gemmatimonadaceae*** and ***Mortierella*** were strongly correlated with lipid metabolites in ***Panax notoginseng***, ***TK10*** and ***Arthrobacter*** in ***Polygonatum sibiricum***, and nitrogen-containing and aromatic compounds in ***Eutrema wasabia***. Collectively, our findings unravel the microbe-driven mechanisms governing quality formation in understory medicinal plants and provide theoretical support for optimizing understory cultivation regimes, sustaining soil fertility, and mitigating continuous monocropping obstacles in eco-friendly forest-economy systems.

Keywords: Under-forest ***Panax notoginseng***;Under-forest ***Polygonatum sibiricum***; Under-forest ***Eutrema wasabia***; Root exudates; Soil nutrients; Soil rhizosphere microorganisms

1 Introduction

In recent years, traditional Chinese medicinal materials under the forest have become an important

growth point for Yunnan's understory economy. The "14th Five-Year Plan for Under-Forest Traditional Chinese Medicine Industry in Yunnan Province" clearly proposes to expand the planting space of traditional Chinese medicine based on the abundant forest resources in the province [1]. As for the whole country, the authentic production areas of major medicinal herbs such as Panax notoginseng are highly concentrated in the Wenshan Zhuang and Miao Autonomous Prefecture in southeastern Yunnan [2]. However, constrained by continuous cropping obstacles, the production area is accelerating its spread to the periphery of traditional planting areas [3], and Xundian County located in the northeast of Kunming is an emerging carrier of this diffusion process. Quantitative evaluation of the suitability of medicinal herb cultivation in the county, and the use of multi-source spatial data to depict the distribution pattern and evolution trend of suitable areas at all levels, can not only promote local agricultural informatization construction, but also lay the foundation for the long-term sustainable development of medicinal herb cultivation and processing industry [4].

There are two main ways in which plant roots release secretions: physiological release relying on primary metabolism, and passive release independent of metabolic activity[4]. The former ensures the energy and material supply required for plant growth and development [5], while the latter often releases a large amount of secondary metabolites, a considerable portion of which have allelopathic activity. When they continue to accumulate in the soil, they will produce autotoxic effects on the same species or close relatives, becoming an important cause of continuous cropping obstacles [6]. Due to the fact that rhizosphere microorganisms rely mainly on secretions as their carbon and energy sources, the composition characteristics of secretions directly shape the quantity and community composition of rhizosphere microorganisms [7]. Under continuous cropping conditions, the accumulation of autotoxic substances year by year can disrupt the balance of microbial communities and inhibit soil enzyme activity [8], while the weakening of enzyme activity limits the nutrient acquisition ability of medicinal materials, further exacerbating the residual autotoxic substances and forming a vicious cycle of “accumulation-imbalance-re-accumulation” [9-10]. Research pointed out that there is a bidirectional regulatory relationship between root exudates and rhizosphere environment [11]: environmental conditions affect the output of exudates, which in turn modify the environment itself. In summary, root exudates are essentially the hub of information and material exchange between plants, soil, and microorganisms [12]: their input can alter soil physicochemical properties and microbial structure [13], and changes in microbial structure in turn affect the function of soil enzyme systems[14], leading to systematic evolution of rhizosphere microecology; The combined inhibitory effect of autotoxic substances on plant growth constitutes the ecological basis for the occurrence of continuous cropping obstacles in medicinal plants [15].

The rhizosphere microbial community plays an irreplaceable regulatory role in maintaining soil health and supporting crop productivity, and its status directly affects plant stress resistance and final yield [16]. For medicinal plants, the imbalance of rhizosphere microbial structure is often a precursor to the outbreak of soil-borne diseases such as root rot and the aggravation of continuous cropping obstacles [17]. The understanding of how root exudates shape soil microbial communities in understory planting as a new mode of medicinal herb production is currently insufficient [18]. Clarifying this issue not only helps to reveal the microbial ecological evolution laws during the growth process of understory medicinal materials, but also provides theoretical support for the scientific utilization of understory medicinal material resources, soil quality maintenance, and ecological benefits improvement [19]. In addition, the relevant conclusions also have reference significance for the standardized cultivation of

traditional Chinese medicine, ecosystem protection, and soil health management [20].

2 Materials and methods

2.1 Overview of the test site

The experimental site was located in Yunnan Agricultural University Experimental Demonstration Base for Understory Chinese Materia Medica Planting, Xundian County, Kunming City, Yunnan Province, China. The study area has a subtropical monsoon climate with obvious rainy and dry seasons, the altitude of the study area is 2210 m, and the soil is red loam acidic soil. The average annual rainfall is 1,254mm, and it is mostly concentrated in May-December, with sufficient sunshine and large temperature difference, and the average annual temperature is 14.68℃℃, the highest temperature is 37.06℃, and the lowest temperature is 2.53℃. The main trees in the test area were *Pinusyunnanensis*, with a closure degree of 0.7, an average height of 17.5 m, and an average diameter at breast height (Dbh) of 27 cm. The understory shrubs were *Hypericum monogynum, Schima wallichii, Vacciniumbracteatum,* and herbaceous plants mainly include fragrant *Isodon amethystoides*, *Ageratina adenophora* and *Oplismenus compositus*.

2.2 Experimental design and sampling methods

This study used dry season natural forest land (DCK) as the control group, and selected understory forests planted with ***Panax notoginseng***, ***Polygonatum sibiricum***, and ***Eutrema wasabia*** as the research objects to analyze their soil characteristics. Sampling was conducted during the dry season of 2025, including natural forest land (DCK) during the dry season, understory ***Panax notoginseng*** plantation forest land (DPN) during the dry season, understory ***Polygonatum sibiricum*** plantation forest land (DPS) during the dry season, and understory ***Eutrema wasabia*** plantation forest land (DEW) during the dry season. The sample collection depth is 0-20 cm soil layer, and a total of 15 soil samples were collected. Before sampling, the sampling tool should be sterilized at high temperature. After collection, the soil sample should be immediately placed in a sterile sealed bag, stored at -20 ℃, and quickly brought back to the laboratory. Each soil sample is divided into two parts, one part is used for determining soil microbial community characteristics, and the other part is ground and sieved after air drying for determining soil physical and chemical properties.

2.3 Determination of physical and chemical properties of soil

The determination of key soil nutrient properties was conducted using a series of established analytical methods. Total nitrogen was quantified via the Kjeldahl method, which involved an initial digestion of the sample with concentrated sulfuric acid, followed by automated analysis. Total phosphorus was determined by first digesting the samples with a perchloric acid-sulfuric acid mixture, with the resulting solution then analyzed using a continuous flow analyzer. For the measurement of total potassium, a sodium hydroxide alkali fusion-flame photometry method was employed; this procedure consisted of high-temperature fusion of the sample with NaOH, followed by the quantification of potassium concentration using a flame photometer to measure the element's characteristic spectral radiation. The content of available phosphorus was ascertained by leaching the soil with a sodium bicarbonate solution, after which the extract was also measured using a continuous flow analyzer. Finally, available potassium was determined by leaching the samples with an

ammonium acetate solution, and the concentration in the extract was subsequently quantified using flame photometry.

2.4 Measurement of root exudates

Accurately weigh 100mg of the sample and place it in a 2mL centrifuge tube. Add one 6mm grinding bead. Extract with 800 μ L methanol water (4:1, v/v) solution containing four internal standards (such as L-2-chlorophenylalanine 0.02mg/mL). The sample was first frozen and ground for 6 minutes (-10 ℃, 50Hz), and then subjected to low-temperature ultrasound for 30 minutes (5 ℃, 40kHz). After allowing the extract to stand at -20 ℃ for 30 minutes, centrifuge at 4 ℃ and 13000g for 15 minutes, and transfer the supernatant to an injection bottle containing an inner liner for testing.

Chromatographic separation: 3 μ L of the sample was separated on a BEH C18 column (100mm×2.1mm i.d., 1.7 μ m) at a flow rate of 0.40mL/min and column temperature of 40 ℃. Mobile phase A is a 0.1% formic acid aqueous solution (containing 2% acetonitrile), and phase B is 0.1% formic acid acetonitrile. Gradient elution program: 0-0.5min, phase B 2%; 0.5-7.5 minutes, phase B increases to 35%; 7.5-13 minutes, phase B increases to 95%; 13-14.4 minutes, phase B maintains 95%; 14.4-14.5 minutes, phase B decreases to 2%; 14.5-16 minutes, phase B is at 2% equilibrium. Mass spectrometry collection: positive and negative ion switching scanning, m/z 70-1050。 Ion source parameters: positive and negative voltage 3500V/-3000V, sheath gas 50psi, auxiliary gas 13psi, temperature 450 ℃. The collision energy adopts a 20-40-60V step mode, with MS1/MS2 resolution set to 70000/17500.

2.5 Determination of soil microbial communities

For total genomic DNA extraction from microbial communities, DNA extraction was first performed according to the instructions of the E.Z.N.A.® soil DNA kit (Omega Bio-tek, Norcross, GA, U.S.). After extraction, the quality of the DNA was checked using 1% agarose gel electrophoresis. During electrophoresis, DNA samples should form a clear single band, indicating that the DNA is not degraded and that there are no impurities in the sample. The integrity of the DNA was confirmed by observation at 260 nm using a UV transilluminator. After electrophoresis, the concentration and purity of the DNA was determined using a NanoDrop2000 (Thermo Fisher Scientific, USA). The ideal A260/A280 ratio should be between 1.8 and 2.0, which indicates good DNA purity. Using the extracted DNA described above as a template, the upstream primer 338F (5'-ACTCCTACGGGGAGGCAGCAG-3') carrying the Barcode sequence and the downstream primer 806R (5'-GGACTACHVGGGTWTCTAAT-3') were used for PCR amplification of the V3-V4 variable region of the 16S rRNA gene. Downstream primer (5uM) 0.8 μL, TransStart FastPfu DNA polymerase 0.4 μL, template DNA 10 ng, make up to 20 μL. Amplification procedure was as follows: 95 ℃ pre-denaturation for 3min, 27 cycles (95 ℃ denaturation for 30s, 55 ℃ annealing for 30s, 72 ℃ extension for 30s), and then 72 ℃ stabilization and extension for 10min. Finally, it was stored at 4℃ (PCR instrument: ABI GeneAmp® 9700). The PCR products were recovered on a 2% agarose gel, purified using the PCR Clean-Up Kit (China), and quantified using Qubit 4.0 (Thermo Fisher Scientific, USA).

The purified PCR products were used for library construction using NEXTFLEX Rapid DNA-Seq Kit: (1) splice linkage; (2) removal of splice self-associated fragments by magnetic bead screening; (3) enrichment of library templates by PCR amplification; and (4) recovery of PCR products by magnetic beads to obtain the final library. Sequencing was performed using Illumina PE300/PE250 platform (Shanghai Meiji Biomedical Technology Co., Ltd.).

2.6 Data processing and analysis

Excel 2016 was used for data organization, and SPSS Statistics 24.0 one-way analysis of variance (ANOVA, LSD, $P<0.05$) was used to analyze the differences between different treatments. GraphPad Prism 9.5 was used for plotting.

2.7 Plant material identification and voucher specimens

The three medicinal plant materials used in this study, ***Panax notoginseng*** **,** ***Polygonatum sibiricum*** **,** and ***Eutrema wasabia,*** were formally identified by Dr. Bo YANG , an expert in plant taxonomy. Voucher specimens of ***Panax notoginseng, Polygonatum sibiricum,*** and ***Eutrema wasabia*** were deposited at the Herbarium of Southwest Forestry University (SWFU), Kunming, Yunnan, China, under accession numbers SWFU2025-1087, SWFU2025-1088, and SWFU2025-1089, respectively.

3 Result

3.1 Analysis of root secretion profiles in understory medicinal plants

3.1.1 Dissimilarity and PCA analysis of root secretions

Compared with the control group that was not planted during the dry season, the re were 355, 241, and 236 significantly different metabolites of ***Panax notoginseng***, ***Eutrema wasabia***, and ***Polygonatum sibiricum***, respectively, in the understory during t he dry season(Figure 1A). During the dry season, there are a total of 127 significant differential metabolites between ***Panax notoginseng*** and ***Eutrema wasabia***, including L-(+)-arginine, L-glutamine, L-isoleucine, deoxyquercetin, 5'-deoxyfluorouridine, N-acety l-D-tryptophan, ortho aminobenzoic acid, L-glutamic acid, etc. During the dry season, there are 144 common differential metabolites between ***Panax notoginseng*** and ***Polygo natum sibiricum***, mainly including tridecylglycine, valine methionine, light fruit grass naphthalene, 2-hydroxy-6-pentadecanoic acid, 1-dehydro-[6]-gingeredione, N-lauroyl glyc ine, deoxymalic acid, L-leucine, L-glutamic acid, creatinine, L-histidine, anthranilic aci d, apigenin 7- [rhamnosyl-(1->2)-galacturonic acid], etc. During the dry season, there are 122 common differential metabolites between ***Eutrema wasabia*** and ***Polygonatum s ibiricum***, including tetrahydropalmatine, cotinine glucuronide, callus hormone, nifedipin e, dehydrogingerone, niacin, antibiotic SB 202742, 10 hydroxycamptothecin, 5-deoxyrib ose-1-phosphate, sucrose, and p-phenylpropanoid. In addition, there are a total of 89 i dentical differential metabolites among the three compared to those not planted during the dry season, mainly including phenylglucuronide, 3-(3-hydroxyphenyl) propionic ac id (9R,10S,12Z)-9, 10-dihydroxy-8-oxo-12-octadecenoic acid, β- glutamyl-L-glutamic a cid, etc.

In order to accurately analyze the differences in metabolites of different understory Chinese medicinal materials, as shown in (Figure 1B), orthogonal partial least squares discriminant analysis (OPLS-DA) was used. The analysis results showed that different sample

groups (DEW, DPS, DPN, DCK) exhibited significant separation trends in component 1 (24% explanatory power) and component 2 (16.3% explanatory power), indicating significant differences in metabolite or molecular composition among the groups. Therefore, it can be concluded that the metabolites of ***Panax notoginseng***, ***Eutrema wasabia***, and ***Polygonatum sibiricum*** in the understory during the dry season show significant differences compared to the non planted group.

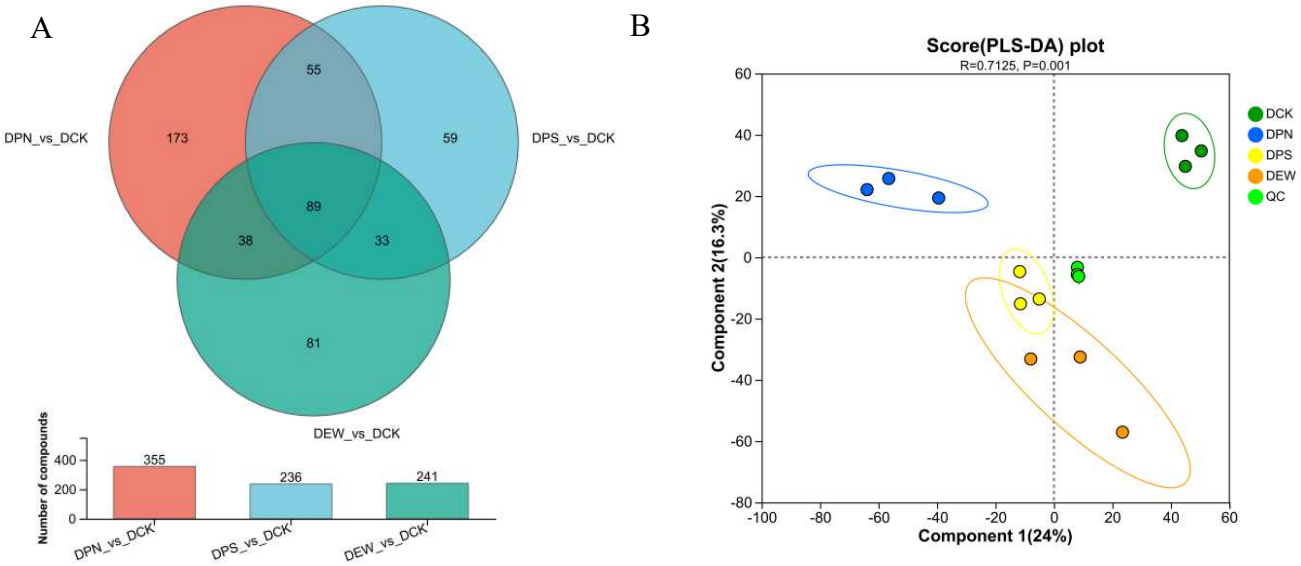


Figure 1 Comparative analysis of root secretions from understory medicinal plants**.** (A) Venn diagram of root secretion components. (B) PCA component analysis (PCA) of root secretions.

3.1.2 Classification of HMDB compounds in root secretions of understory medicinal plants

Root secretions of ***Panax notoginseng***, ***Polygonatum sibiricum***, and ***Eutrema wasabia*** were identified separately by LC-MS.

During the dry season, a total of 355 substances were detected in the root exudates of ***Panax notoginseng***, mainly including lipids and lipid like molecules, organic acids and their derivatives, organic oxygen compounds, phenylpropanoids and polyketones, others, organic heterocyclic compounds, benzene compounds, lignans and neolignans and related compounds, organic nitrogen compounds, nucleosides and nucleotides and their analogues, alkaloids and their derivatives, hydrocarbon derivatives and hydrocarbons. (Figure 2A) shows these substances, Among them, lipids and lipid like molecules, organic acids and their derivatives, organic oxygen compounds, phenylpropanoids and polyketones, and others (with relative contents of 35%, 15.42%, 10.42%, 14.58%, and 0.42%), organic heterocyclic compounds, benzene compounds, lignin and new lignin and related compounds, organic nitrogen compounds, nucleosides and nucleotides and their analogues, alkaloids and their derivatives, hydrocarbon derivatives, and fatty hydrocarbons have relatively low contents, accounting for 0.39% -4.24%;

A total of 236 substances were detected in the root exudates of ***Polygonatum sibiricum*** during the dry season, mainly including lipids and lipid like molecules, organic acids and derivatives, organic oxygen compounds, organic heterocyclic compounds, phenylpropanoids and polyketones, unusable, benzene like compounds, lignin, new lignin and its related compounds, organic nitrogen compounds, nucleotides, nucleosides and analogues, derivatives

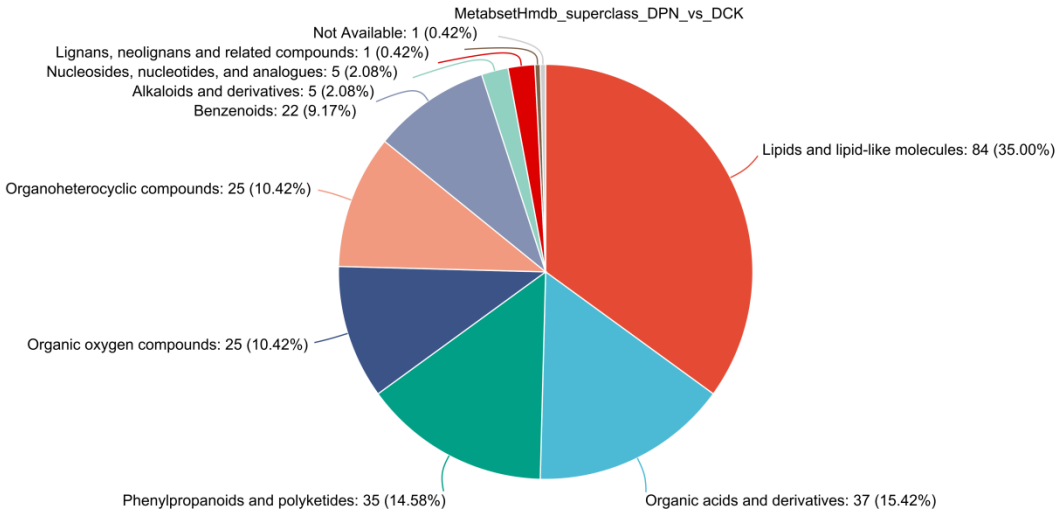
of hydrogen containing compounds, hydrogenated carbon compounds, etc. (Figure 2B) shows that lipids and lipid like molecules account for the largest proportion, reaching 26.32%. Following closely behind are organic acids and derivatives, organic heterocyclic compounds, phenylpropanoids, and polyketones, accounting for 16.96%, 12.28%, 14.62%, and 8.77%, respectively. However, the proportion of hydrogenated carbon compounds, derivatives of hydrogen containing compounds, nucleotides, nucleosides and analogues, organic nitrogen compounds, lignin, new lignin and related compounds, and benzene compounds is relatively low, accounting for 0.58% -4.09%;

During the dry season, 241 substances were detected in the root exudates of ***Eutrema wasabia***, mainly including lipids and lipid like molecules, phenylpropanoids and polyketones, organic heterocyclic compounds, organic acids and their derivatives, benzene compounds, organic oxygen compounds, alkaloids and their derivatives, hydrocarbon derivatives, nucleosides and nucleotides and their analogues, hydrocarbons and organic nitrogen compounds. (Figure 2C) shows that the relative content of lipids and lipid like molecules, phenylpropanoids and polyketones is the highest, reaching 28.40% and 15.98% respectively, followed by organic heterocyclic compounds, organic acids and their derivatives, benzene compounds and organic oxygen compounds (relative content of 12.43%, 14.79%, 8.88% and 10.65%), alkaloids and their derivatives, hydrocarbon derivatives, nucleosides and nucleotides. The relative content of its analogues, hydrocarbons, and organic nitrogen compounds is relatively low, accounting for 1.18%.

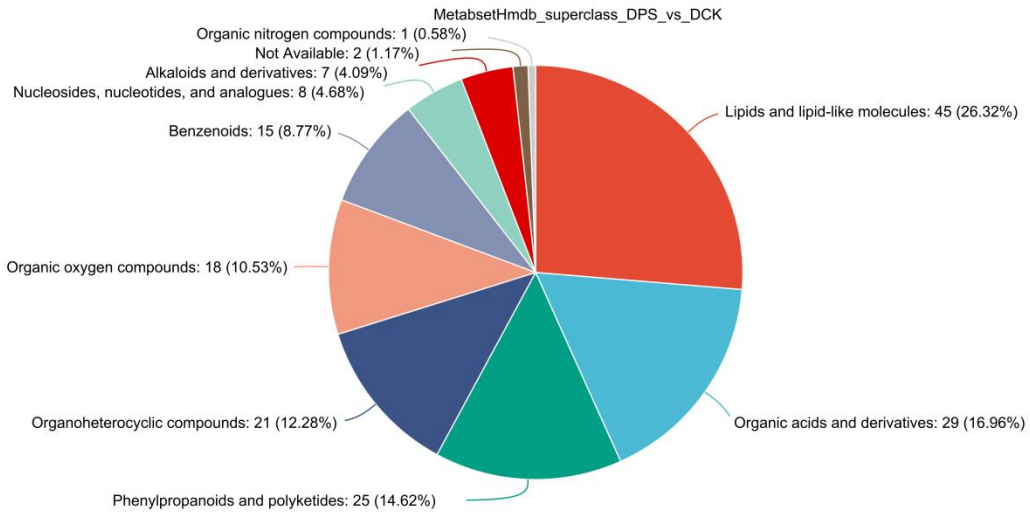
The HMDB ultrasound classification results of differential metabolites in root exudates of ***Panax notoginseng***, ***Polygonatum sibiricum***, and ***Eutrema wasabia*** indicate that there are similarities and differences in the chemical composition of the three medicinal plants. In terms of commonality, lipids and lipid molecules account for the largest proportion in ***Panax notoginseng*** (35.00%), ***Polygonatum sibiricum*** (26.32%), and ***Eutrema wasabia*** (28.40%), indicating that lipid compounds play an important role in their root metabolic response. Another common feature is that the proportion of organic acids and their derivatives in the three plants is relatively high, with ***Panax notoginseng*** accounting for 15.42%, ***Polygonatum sibiricum*** accounting for 16.96%, and ***Eutrema wasabia*** accounting for 14.79%. In addition, the proportion of organic oxygen-containing compounds (10.42%, 10.53%, and 10.65%, respectively) and phenylpropane and polyketide compounds (14.58%, 14.62%, and 15.98%, respectively) in the three plants is similar, indicating that these substances may play a protective role in physiological functions such as allelopathic defense and antioxidant. In terms of variability, there are significant differences in the types and proportions of substances among the three species. In terms of the total number of differential metabolites, ***Panax notoginseng*** has the strongest chemical response (240 species), while ***Polygonatum sibiricum*** and ***Eutrema wasabia*** have 171 and 169 species, respectively. Especially in terms of component distribution, the proportion of lipids in ***Panax notoginseng*** (35.00%) is significantly higher than that in ***Polygonatum sibiricum*** (26.32%) and***Eutrema wasabia*** (28.40%), while the proportion of alkaloids in ***Polygonatum sibiricum*** (4.09%) is higher than that in ***Panax notoginseng*** (2.08%) and ***Eutrema wasabia*** (1.18%). In addition, the detection of unique organic sulfur compounds (1.78%) in ***Eutrema wasabia*** is highly consistent with its metabolic characteristics as a cruciferous plant rich in glucosinolates. These differences indicate that the three plants may have different physiological functions and ecological adaptation mechanisms in terms of root secretion strategies and adaptation strategies.

In summary, the root exudates of ***Panax notoginseng***, ***Polygonatum sibiricum***, and ***Eutrema wasabia*** have a complex composition and share similarities in lipid and organic acid components. However, there are significant differences among the three plants in terms of the types and proportions of components, especially in the content of lipids, alkaloids, and organic sulfur compounds. These differences may be closely related to their phylogenetic background, ecological functions, and rhizosphere adaptation strategies.

A



B



C

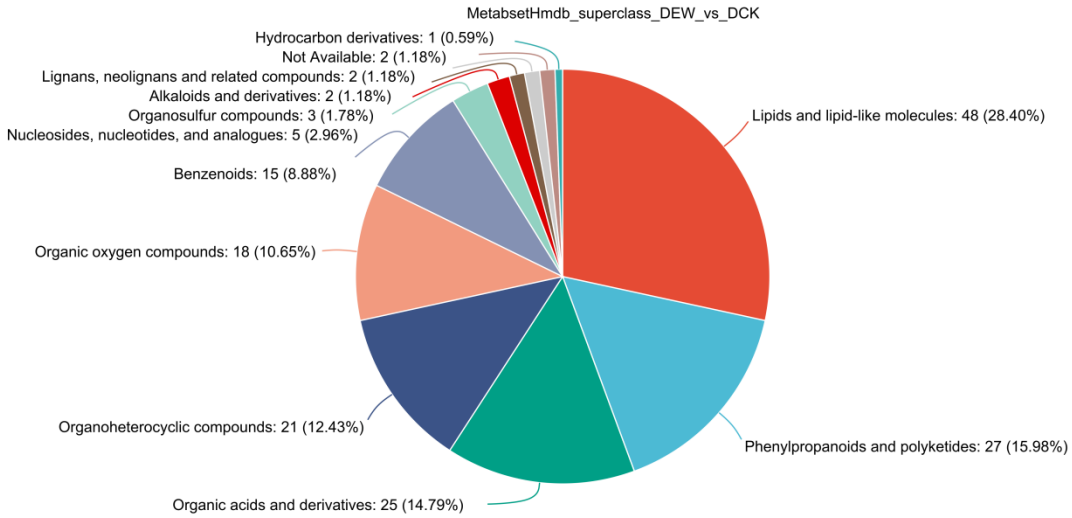


Figure 2 Classification of HMDB compounds in root secretions of understory medicinal plants. (A) HMDB compound classification in ***Panax notoginseng*** root secretions. (B) HMDB compound classification in ***Polygonatum sibiricum*** root secretions. (C) HMDB compound classification in ***Eutrema wasabia*** root secretions.

3.1.3 KEGG pathway enrichment analysis of root secretions in understory medicinal plants

The results of metabolic pathway enrichment analysis revealed the differential effects of different understory planting modes on the root metabolic network of medicinal plants. Compared with the control (DCK), the metabolic disturbance of DPN treatment was the most significant, with a total of 71 pathways enriched, of which 23 ($P<0.05$) reached a significant level. The pathway with the highest enrichment ratio (ER) is plant hormone signal transduction (ER ≈ 0.165, $P<0.05$), followed by aminoacyl tRNA biosynthesis (ER≈0.155, $P<0.001$) and citrate cycle (ER≈0.15, $P<0.01$), indicating that Panax notoginseng enhances protein translation, energy metabolism, and hormone regulation simultaneously in the understory environment. Amino acid metabolism pathways are widely activated, including alanine, aspartate, and glutamate metabolism (ER≈0.145), arginine biosynthesis, phenylalanine metabolism, arginine and proline metabolism, and tryptophan metabolism; The significant enrichment of glutathione metabolism and ABC transporters further suggests their enhanced antioxidant and substance transport capabilities. It is worth noting that DPN also significantly enriches defense related pathways such as glucosinolate biosynthesis, flavonoid biosynthesis, and biosynthesis of various plant secondary metabolites, reflecting its unique chemical defense regulatory mechanism(Figure 3A).

DPS treatment enriched a total of 52 pathways, of which 16 ($P<0.05$) were significant, and their enrichment patterns were both common and clearly differentiated from DPN. The highest enrichment levels are in plant hormone signal transduction (ER≈0.17) and nucleotide metabolism (E ≈0.16), followed by ABC transporters and pyrimidine metabolism, indicating that the metabolic adaptation of Polygonatum sibiricum is more focused on genetic material turnover, nucleic acid synthesis, and transmembrane material transport. Similar to DPN, DPS

also significantly activates amino acid related pathways such as galactose metabolism, valine, leucine, and isoleucine biosynthesis, aminoacyl tRNA biosynthesis, and alanine, aspartate, and glutamate metabolism; At the same time, characteristic secondary metabolic pathways such as vitamin B6 metabolism, linoleic acid metabolism, Tropane, piperidine, and pyridine alkaloid biosynthesis, and indole alkaloid biosynthesis are also enriched. The activation of alkaloid synthesis pathways corresponds to the higher proportion of alkaloids in the root exudates, reflecting the unique chemical ecological strategy of Polygonatum sibiricum(Figure 3B).

In contrast, the metabolic disturbances of DEW treatment were relatively concentrated, with a total of 44 pathways enriched, of which 8 ($P<0.05$) were significant and clearly biased towards lipid and secondary metabolism. The enrichment ratio of linoleic acid metabolism was the highest among all treatments (ER≈0.18, $P<0.001$), while galactose metabolism, plant hormone signal transduction, flavonoid biosynthesis, and oxidative phosphorylation were significantly enriched. At the same time, alpha linolenic acid metabolism and betaine biosynthesis were also significantly enriched. biosynthesis of cutin, suberin, and wax (Cutin, suberin, and wax biosynthesis) The activation of pathways indicates that as a cruciferous plant, wasabi is highly dependent on unsaturated fatty acid metabolism and secondary metabolism of phenols and flavonoids in the understory environment to cope with low light and biological stress(Figure 3C).

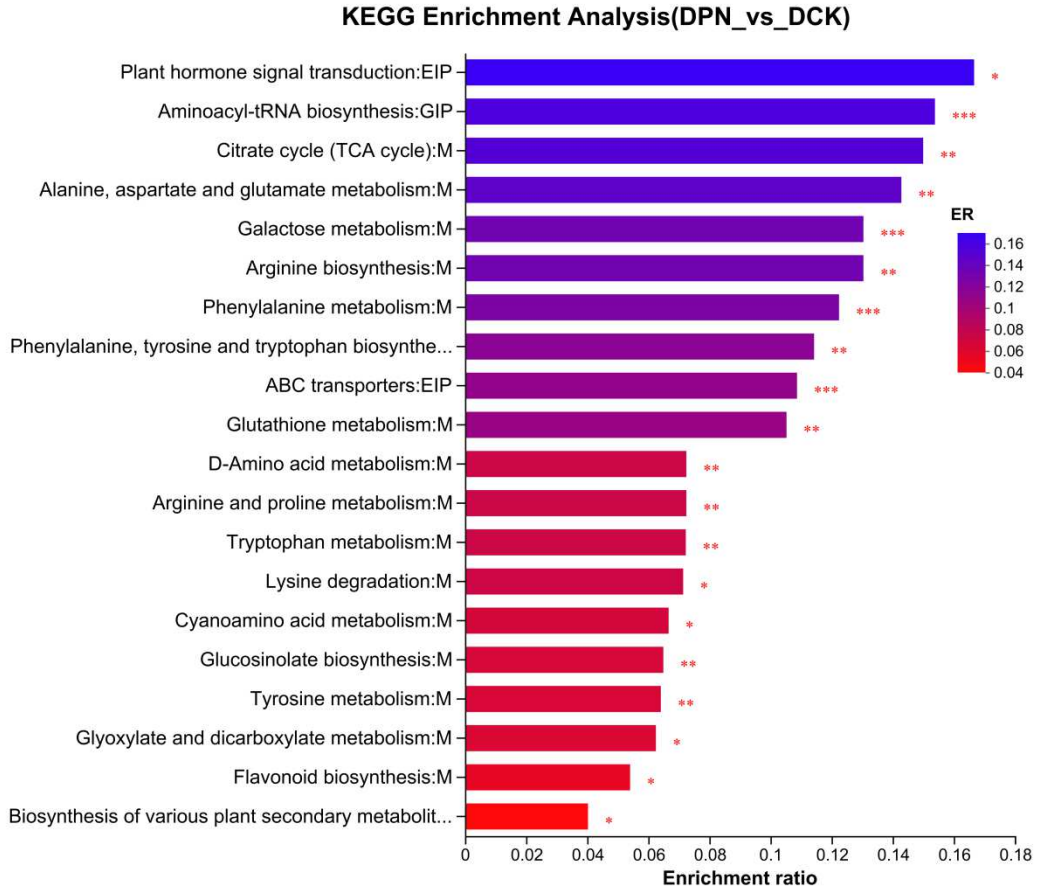
DPN vs DPS (difference between dry season ***Panax notoginseng*** and dry season ***Polygonatum sibiricum***) significantly enriched pathways ($P<0.05$, red bubble): Aminoacyl tRNA biosynthesis: Rich Factor ≈ 0.15, Number=8 (largest bubble), which is the most significant pathway in this group. Aminoyl tRNA is a key intermediate product in protein synthesis, suggesting that the difference between DPN and DPS may be closely related to protein translation efficiency or amino acid metabolism. Arginine and proline metabolism: Rich Factor ≈ 0.12, Number=7, involving nitrogen metabolism and osmotic regulation, may be associated with stress response (such as drought, salt stress). Glutamate metabolism: Rich Factor ≈ 0.1, Number=6, is a central metabolic pathway that connects carbon metabolism and nitrogen metabolism, indicating differences in carbon and nitrogen balance between DPN and DPS. Other significant pathways include beta alanine metabolism, biosynthesis of various plant secondary metabolites, etc., involving small molecule metabolites and secondary metabolism. Non significant pathways (purple bubbles), such as "valine, leucine, and isoleucine degradation", have large P-values and no statistical differences(Figure 3D).

The pathway significantly enriched in DEW vs DPN (difference between dry season ***Eutrema wasabia*** and dry season ***Panax notoginseng***) ($P<0.05$, red bubble): Aminoacyl tRNA biosynthesis: Rich Factor ≈ 0.2, Number=10 (maximum bubble), is the most significant pathway in this group. Consistent with the previous two groups, it emphasizes once again the central role of protein synthesis in the differences between DEW and DPN, which may be a key driving factor for the differences between the two groups. Glycine, serine, and threonine metabolism: Rich Factor ≈ 0.15, Number=9, involving amino acid interconversion and one carbon unit metabolism, is an important source of methyl donors (such as S-adenosylmethionine), indicating differences in amino acid interactions between DEW and DPN. Plant hormone signal transduction: Rich Factor ≈ 0.12, Number=8, is the core pathway

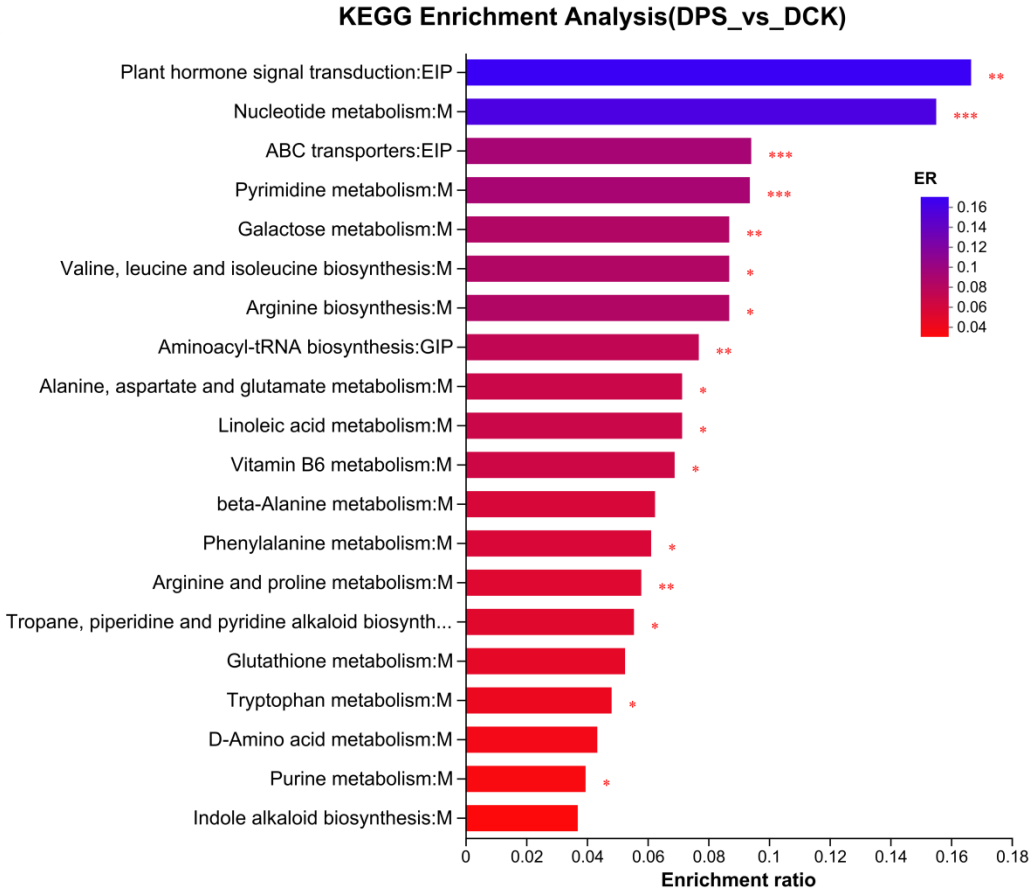
for plants to respond to environmental stimuli such as light, temperature, and hormones, indicating significant differences in hormone signal transduction between DEW and DPN. Other significant pathways include stilbene biosynthesis, terpenoid biosynthesis, etc., which involve the synthesis of secondary metabolites such as resveratrol and terpenoids, and may be related to stress resistance or quality formation. Non significant pathways, such as beta alanine metabolism, have a high P-value and no significant difference(Figure 3E).

The pathway significantly enriched in DPS vs DEW (difference between dry season ***Polygonatum sibiricum*** and dry season ***Eutrema wasabia***) (P<0.05, red bubble): Tryptophan metabolism: Rich Factor ≈ 0.18, Number=7 (larger bubble), is one of the most significant pathways in this group. Tryptophan is an essential amino acid, and its metabolites (such as indoleacetic acid) participate in plant growth regulation (such as rooting and flowering), indicating differences in hormone synthesis or growth and development between DPS and DEW. ABC transporters: Rich Factor ≈ 0.16, Number=6, involved in transmembrane transport of substances (such as ions, drugs, secondary metabolites), may reflect differences in substance exchange capacity between DPS and DEW. Purine metabolism: Rich Factor ≈ 0.14, Number=5, involving the synthesis and breakdown of nucleic acids (DNA/RNA), indicating differences in genetic material metabolism between DPS and DEW. Other significant pathways include D-amino acid metabolism, nucleotide metabolism, etc., which involve amino acid and nucleic acid metabolism. Non significant pathways, such as "Citrulline and arginine metabolism," have a high P-value and no significant difference(Figure 3F).

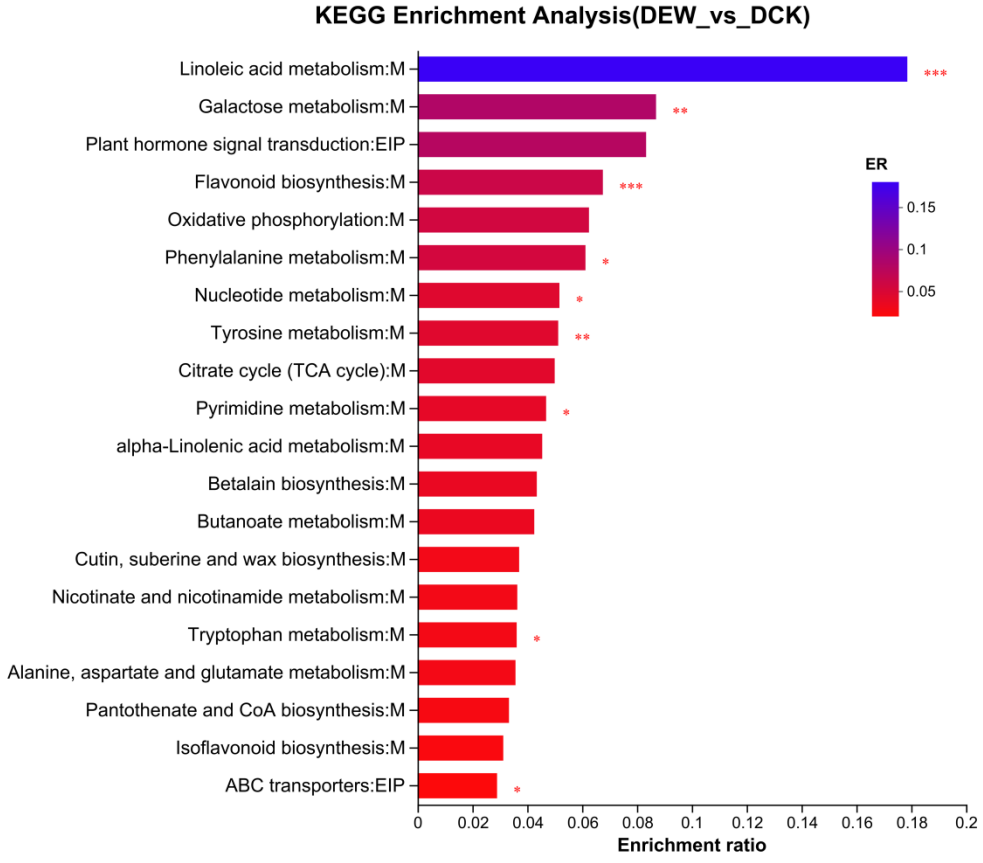
A



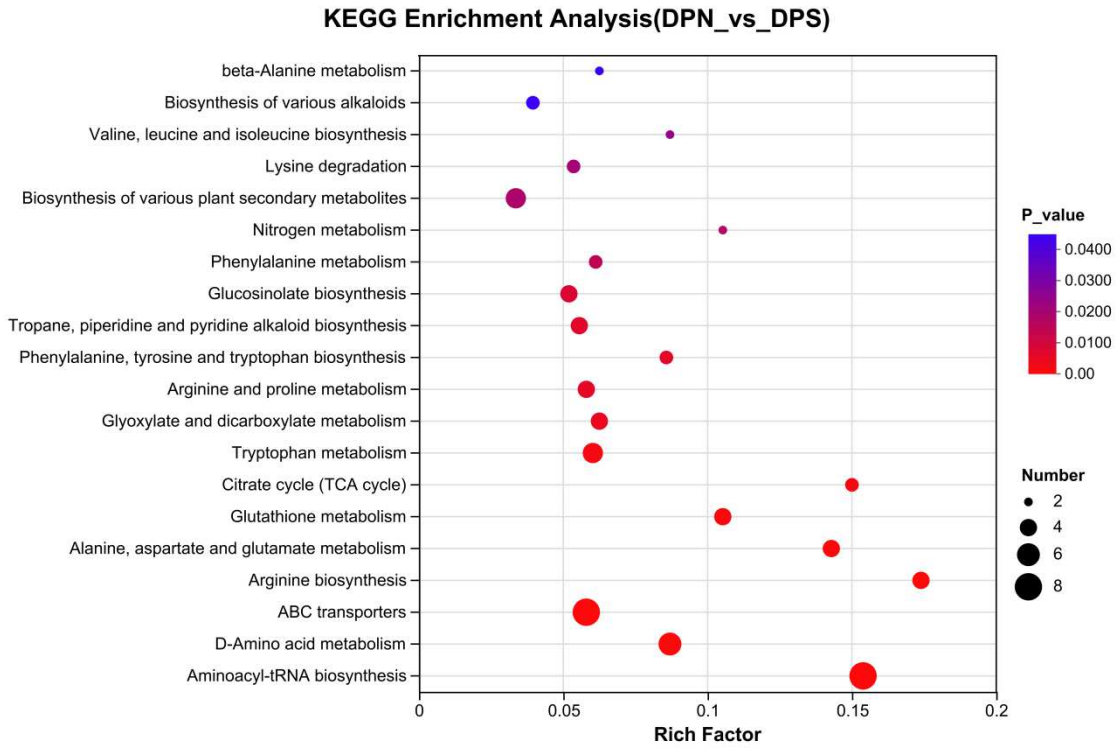
B


KEGG Enrichment Analysis(DPS_vs_DCK)
Plant hormone signal transduction:EIP
Nucleotide metabolism:M
ABC transporters:EIP
Pyrimidine metabolism:M
Galactose metabolism:M
Valine, leucine and isoleucine biosynthesis:M
Arginine biosynthesis:M
Aminoacyl-tRNA biosynthesis:GIP
Alanine, aspartate and glutamate metabolism:M
Linoleic acid metabolism:M
Vitamin B6 metabolism:M
beta-Alanine metabolism:M
Phenylalanine metabolism:M
Arginine and proline metabolism:M
Tropane, piperidine and pyridine alkaloid biosynth...
Glutathione metabolism:M
Tryptophan metabolism:M
D-Amino acid metabolism:M
Purine metabolism:M
Indole alkaloid biosynthesis:M
ER
0.16
0.14
0.12
0.1
0.08
0.06
0.04
0
0.02
0.04
0.06
0.08
0.1
0.12
0.14
0.16
0.18
Enrichment ratio

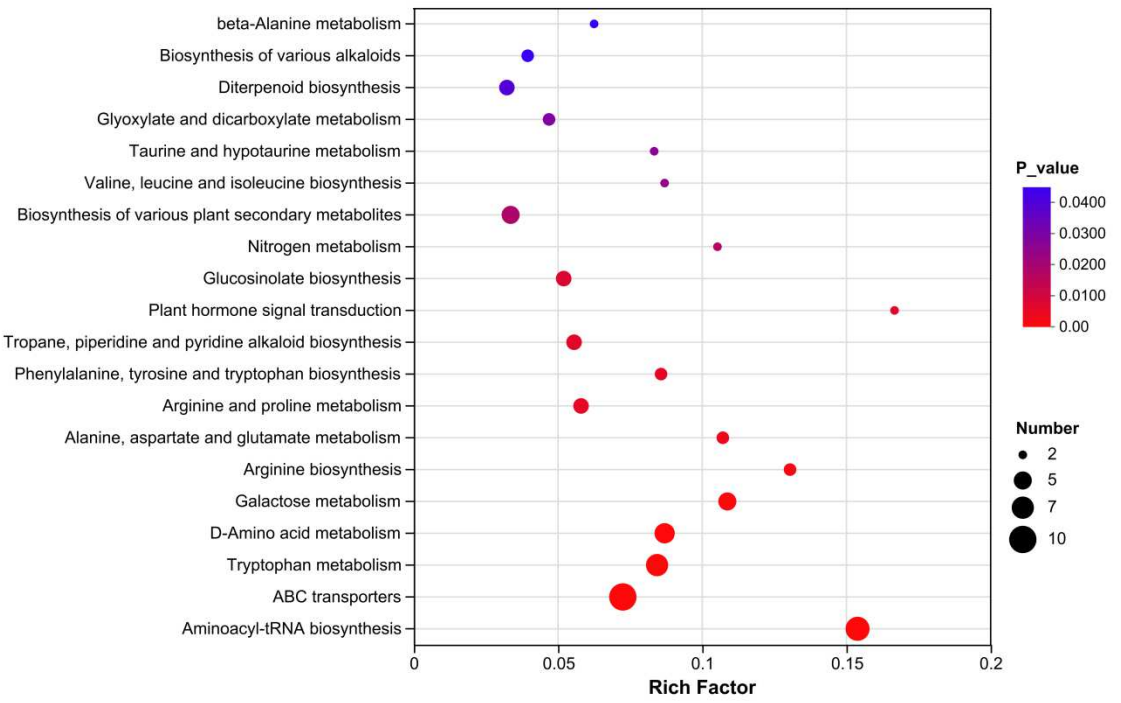
C


KEGG Enrichment Analysis(DEW_vs_DCK)
Linoleic acid metabolism:M
Galactose metabolism:M
Plant hormone signal transduction:EIP
Flavonoid biosynthesis:M
Oxidative phosphorylation:M
Phenylalanine metabolism:M
Nucleotide metabolism:M
Tyrosine metabolism:M
Citrate cycle (TCA cycle):M
Pyrimidine metabolism:M
alpha-Linolenic acid metabolism:M
Betalain biosynthesis:M
Butanoate metabolism:M
Cutin, suberine and wax biosynthesis:M
Nicotinate and nicotinamide metabolism:M
Tryptophan metabolism:M
Alanine, aspartate and glutamate metabolism:M
Pantothenate and CoA biosynthesis:M
Isoflavonoid biosynthesis:M
ABC transporters:EIP
ER
0.15
0.1
0.05
0
0.02
0.04
0.06
0.08
0.1
0.12
0.14
0.16
0.18
0.2
Enrichment ratio

D


KEGG Enrichment Analysis(DPN_vs_DPS)
beta-Alanine metabolism
Biosynthesis of various alkaloids
Valine, leucine and isoleucine biosynthesis
Lysine degradation
Biosynthesis of various plant secondary metabolites
Nitrogen metabolism
Phenylalanine metabolism
Glucosinolate biosynthesis
Tropane, piperidine and pyridine alkaloid biosynthesis
Phenylalanine, tyrosine and tryptophan biosynthesis
Arginine and proline metabolism
Glyoxylate and dicarboxylate metabolism
Tryptophan metabolism
Citrate cycle (TCA cycle)
Glutathione metabolism
Alanine, aspartate and glutamate metabolism
Arginine biosynthesis
ABC transporters
D-Amino acid metabolism
Aminoacyl-tRNA biosynthesis
0
0.05
0.1
0.15
0.2
Rich Factor
P_value
0.0400
0.0300
0.0200
0.0100
0.00
Number
2
4
6
8

E


KEGG Enrichment Analysis(DEW_vs_DPN)
beta-Alanine metabolism
Biosynthesis of various alkaloids
Diterpenoid biosynthesis
Glyoxylate and dicarboxylate metabolism
Taurine and hypotaurine metabolism
Valine, leucine and isoleucine biosynthesis
Biosynthesis of various plant secondary metabolites
Nitrogen metabolism
Glucosinolate biosynthesis
Plant hormone signal transduction
Tropane, piperidine and pyridine alkaloid biosynthesis
Phenylalanine, tyrosine and tryptophan biosynthesis
Arginine and proline metabolism
Alanine, aspartate and glutamate metabolism
Arginine biosynthesis
Galactose metabolism
D-Amino acid metabolism
Tryptophan metabolism
ABC transporters
Aminoacyl-tRNA biosynthesis
0
0.05
0.1
0.15
0.2
Rich Factor
P_value
0.0400
0.0300
0.0200
0.0100
0.00
Number
2
5
7
10

F

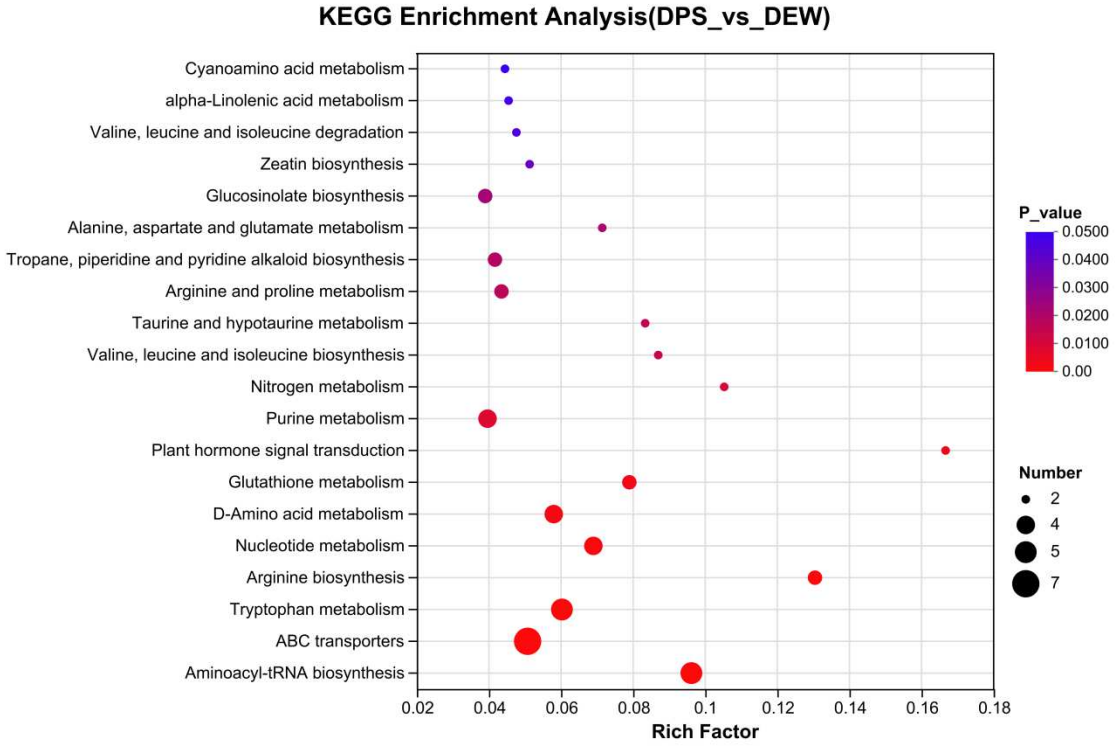


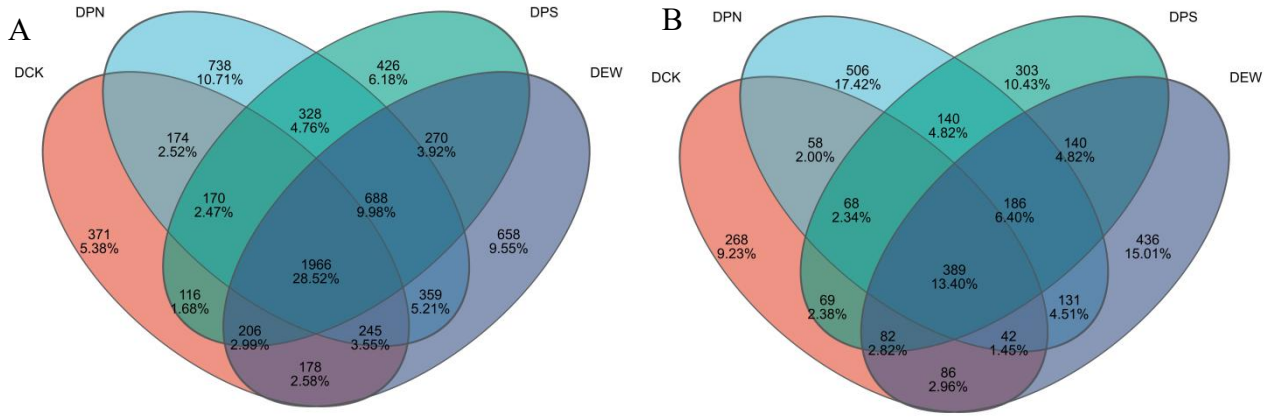
Figure 3 KEGG pathway enrichment analysis of root secretions from understory medicinal plants. (A)Metabolic pathway diagram of significantly enriched secretion differences between understory ***Panax notoginseng*** and non planted. (B)Metabolic pathway diagram showing significant enrichment of differential secretions between understory ***Polygonatum sibiricum*** and non planted.(C) Metabolic pathway diagram of significantly enriched secretion differences between understory ***Eutrema wasabia*** and non planted. (D) Enriched pathways in ***Panax notoginseng*** compared to ***Polygonatum sibiricum***.(E) Enriched pathways in ***Panax notoginseng*** compared to ***Eutrema wasabia***. (F) Enriched pathways in ***Polygonatum sibiricum*** compared to ***Eutrema wasabia***.

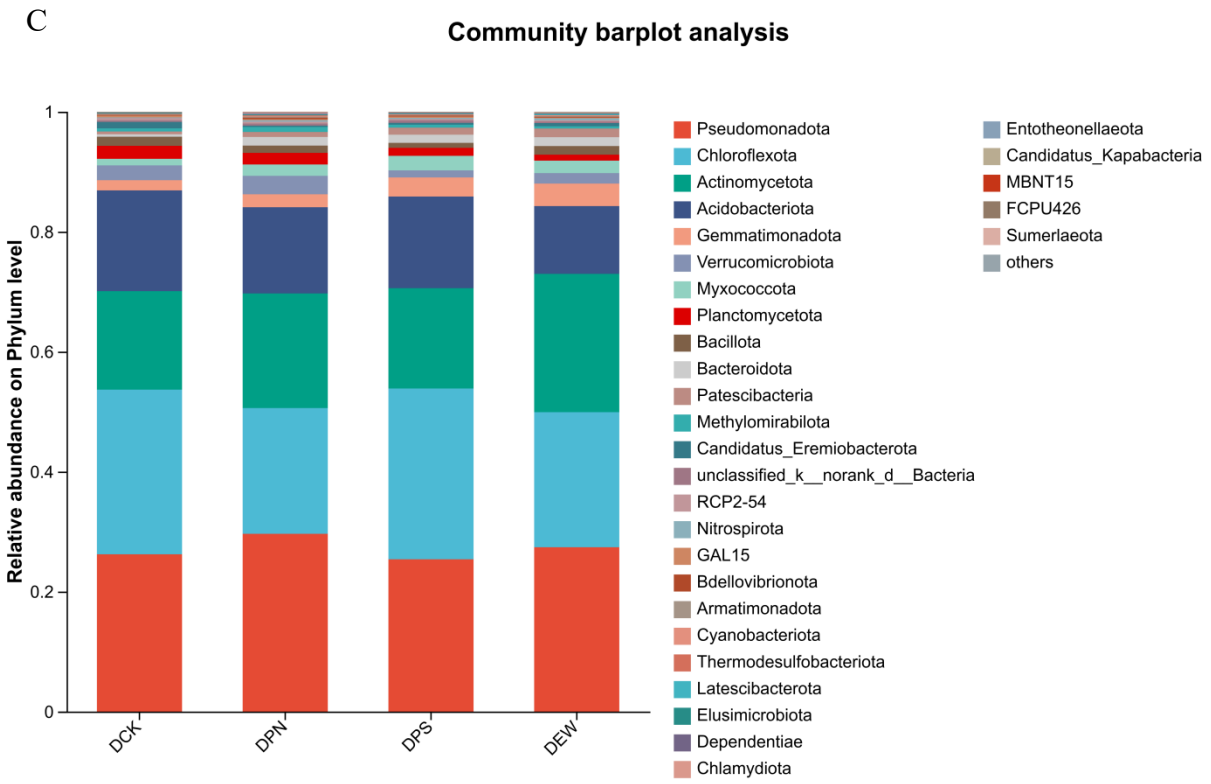
3.2 Community characteristics of inter-root microorganisms in forested Chinese herbal soils

3.2.1 Composition of soil microbial communities in understory medicinal plants

Based on the analysis of OTU distribution and taxonomic abundance of rhizosphere soil microorganisms in four understory medicinal plants, this study revealed the ecological characteristics of soil microbial communities in four groups: DCK, DPN, DPS, and DEW, and their significant differences under different treatments (Figure 3). The Venn diagram results showed that the proportion of four shared OTUs in the bacterial community was as high as 28.52% (1966 individuals), indicating the existence of significant shared dominant bacterial groups under different planting modes. Among them, DCK and DPN had a higher proportion of group specific OTUs (5.38% and 10.71%); In contrast, the proportion of shared OTUs in fungal communities was only 13.40% (368), while the proportion of group specific OTUs in DPN and DEW was higher (17.42% and 15.01%), indicating that fungal communities are more sensitive to different planting patterns, and their distribution heterogeneity is significantly higher than that of bacterial communities

(Figure 4AB). At the phylum classification level, ***Pseudomonas, Acidobacteriota, Chloroflexita,*** and ***Actinomycota*** are the main dominant phyla in bacterial communities. Among them, the relative abundance of Pseudomonas in the planting treatment group (DPN, DPS, DEW) was higher than that in the natural control group (DCK), while ***Acidobacteria*** was relatively enriched in the DCK group. ***Chloroflexita*** and ***Actinomycota*** showed significant differentiation between different treatments ($P<0.05$); ***Ascomycota, Basidiomycota,*** and ***Mortierellomycota*** are the main dominant phyla in the fungal community. The relative abundance of ***Ascomycota*** in the planting group was significantly higher than that in the control group. Ascomycota had the highest proportion (about 55%) in the DPN group, while ***Basidiomycota*** had a significant relative abundance (about 56%) in the control group. ***Mortierellomycota*** was significantly enriched in the DEW group (Figure 4CD). The above results indicate that different planting patterns of medicinal plants under different forests have a significant impact on the structure and abundance of rhizosphere soil bacteria and fungi communities. The response of fungal communities to planting activities is greater than that of bacterial communities, and AM fungal related groups (***Ascomycota***) are enriched in some treatments. This may be closely related to the allelopathic characteristics of root exudates and differences in rhizosphere carbon source input of different medicinal plants, providing important scientific basis for the subsequent analysis of the "variety rhizosphere microbiota medicinal quality" ternary interaction mechanism and the development of functional microbial agents.





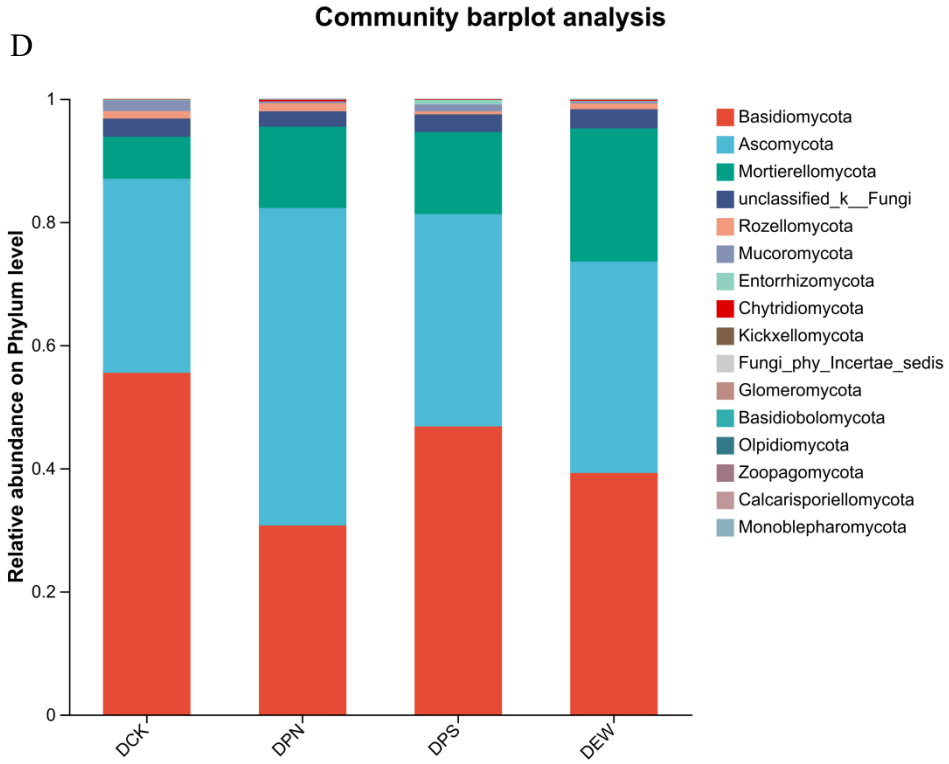


Figure 4 Analysis of soil microbial community composition and relative abundance in understory medicinal plants. (A)Venn diagram of bacterial community composition. (B) Venn diagram of fungal community composition. (C) Relative abundance of bacterial phyla. (D) Relative abundance of fungal phyla.

3.2.2Microbial diversity in soils of understory medicinal plants

Figure 5 shows the Shannon diversity dilution curve of the rhizosphere soil microbial community of medicinal plants under the forest. The relationship between sequencing depth and diversity index reveals the community diversity characteristics of bacteria (Figure 5A) and fungi (Figure 5B) under four treatments (DCK, DPN, DPS, DEW). The bacterial diversity curve (Figure 5A) shows that the Shannon index of the DPN group is the highest (about 4.55), significantly higher than that of the control group DCK (about 4.1) and DEW group (about 4.0), followed by the DPS group (about 4.35), indicating that the planting of Panax notoginseng significantly improves the diversity of rhizosphere bacterial communities; The fungal diversity curve (Figure 5B) showed a similar differentiation pattern, with the DPN group having the highest index (about 6.35), followed by the DPS and DEW groups (about 6.2), and the DCK group having the lowest (about 5.9). Moreover, the fungal diversity of each treatment group was relatively lower than the inter group differences corresponding to bacteria. The dilution curves of the four groups of samples tend to flatten with increasing sequencing depth, indicating that the sequencing depth of 50000 reads has fully covered the microbial communities in the samples. The sequencing data volume is sufficient to reflect the true community structure of each treatment group, and the subsequent diversity analysis results are reliable.

In summary, DPN treatment significantly increased the alpha diversity of rhizosphere soil microorganisms, which may be related to the more complex composition of root exudates in ***Panax notoginseng*** and the provision of richer carbon source substrates for rhizosphere microorganisms; The DCK group had the lowest diversity, reflecting the relatively single input of soil carbon sources in the natural control. Different planting patterns selectively shape microbial community diversity through differences in the rhizosphere microenvironment mediated by root exudates, laying a data foundation for subsequent predictions of rhizosphere microbial function and "variety microbe" matching layouts.

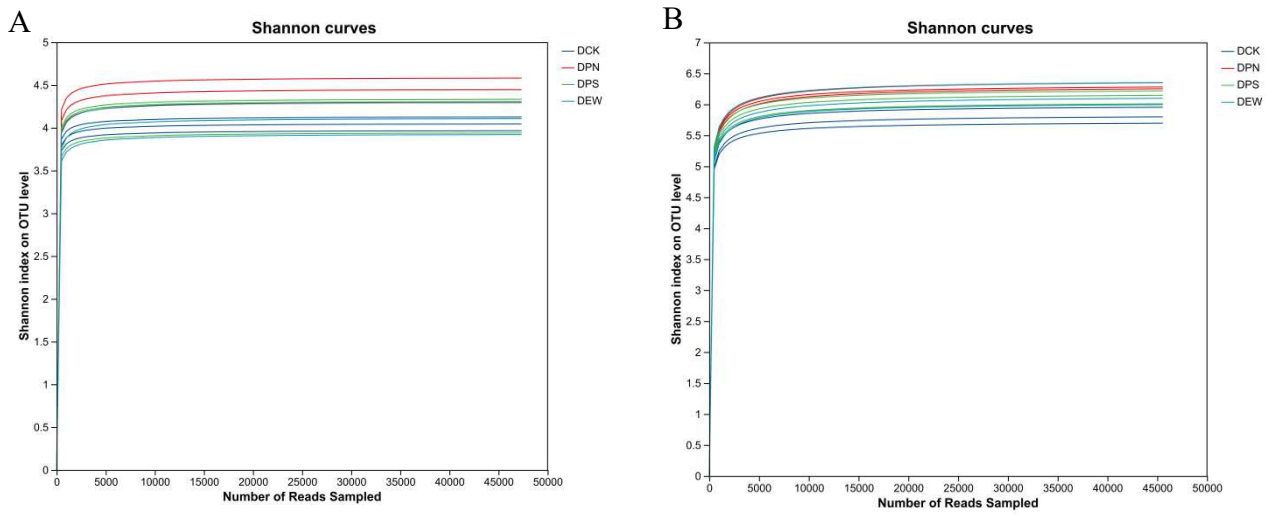


Figure 5 Microbial diversity rarefaction curves for understory medicinal plants. (A) Bacterial diversity rarefaction curves. (B) Fungal diversity rarefaction curves.

The principal coordinate analysis (PCoA) based on OTU level and Bray Curtis algorithm was used to evaluate the β diversity of soil microbial communities under four treatments. The results showed that the community structures of bacteria (Figure 6A) and fungi (Figure 6B) showed significant differentiation among the treatment groups. The PCoA results showed that the first and second principal axes (PC1 and PC2) of the bacterial community explained 17.16% and 13.14% of the variation, respectively (cumulative 30.30%), while the PC1 and PC2 of the fungal community explained 18.13% and 13.78% of the variation, respectively (cumulative 31.91%). The ANOSIM test further confirmed the statistical significance of the inter group differences (bacteria: R=0.4784, P=0.002); Fungi: R=0.48765, P=0.001). In the bacterial community (Figure 6A), the DPN group samples independently clustered along the positive direction of PC1, with the most obvious separation from the DCK group. The DEW group samples were distributed in the positive direction of PC2 and clustered well within the group, while the DPS group and DCK group partially overlapped in the negative direction of PC1, indicating a high similarity in the bacterial community structure between the two groups, which may reflect the relatively mild disturbance of Huangjing root secretion on the bacterial community. In the fungal community (Figure 6B), the DPN group samples significantly separated and independently clustered along the positive direction of PC1, with tight clustering within the group. The DCK group clustered along the negative direction of PC1, while the DEW group extended and distributed along the negative direction of PC2 with relatively large intra group dispersion. The DPS group was located in the coordinate center area and distributed more dispersed, indicating that the inter individual variation of fungal community structure under Polygonatum sibiricum cultivation was more significant, and different treatments had a more significant impact on fungal community composition than bacteria.

In summary, the PCoA and ANOSIM results jointly confirm that different understory medicinal plant planting patterns significantly reshape the community structure of rhizosphere soil microorganisms, and fungal communities are more sensitive to planting treatments than bacteria. This is consistent with the low proportion of OTUs shared by fungi in the Venn diagram mentioned above, providing evidence at the beta diversity level for the subsequent analysis of the interaction relationship between planting patterns, rhizosphere microorganisms, and soil function.

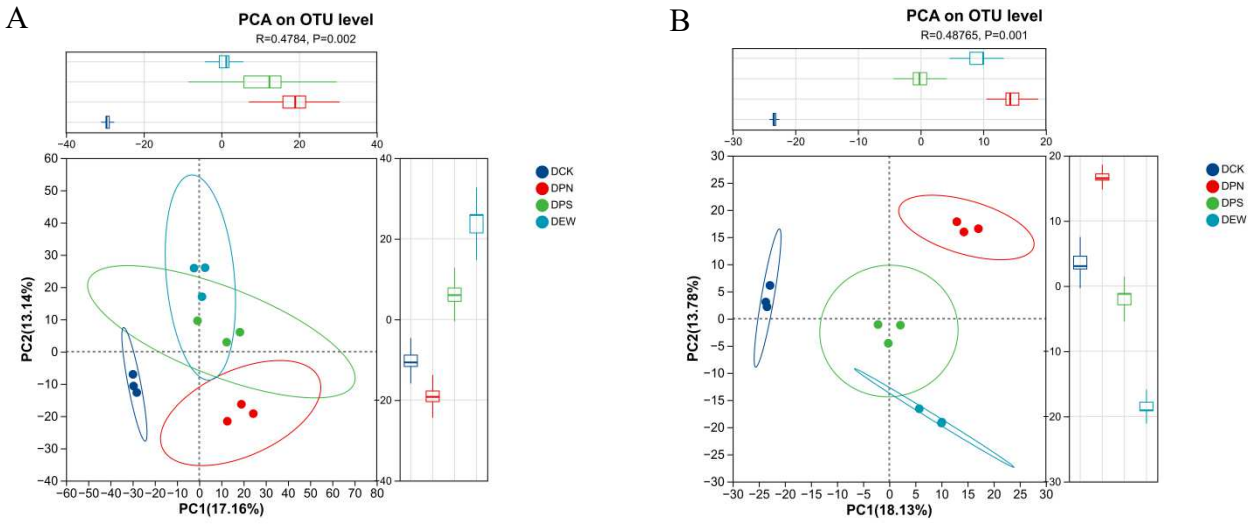


Figure 6 PCoA and ANOSIM analysis of soil microbial communities at the OTU level. (A) PCoA

results for bacterial communities. (B) PCoA results for fungal communities.

3.2.3 Correlation between soil physicochemical properties and microbial communities in understory medicinal plants

Figure 7 reveals the correlation between soil physicochemical properties (pH, organic matter SOM, available phosphorus AP, available potassium AK, total nitrogen TN, total phosphorus TP, and soil moisture SMC) and dominant bacterial (Figure 7A) and fungal (Figure 7B) populations at the genus level through redundancy analysis (RDA). The RDA results showed that the first two constraint axes of bacterial community (RDA1 and RDA2) explained 35.13% and 24.02% of the variation, respectively (cumulative 59.15%), while the RDA1 and RDA2 of fungal community explained 32.40% and 14.72% of the variation, respectively (cumulative 47.12%), indicating that soil physicochemical factors have strong explanatory power for microbial community variation under different planting modes. In the bacterial community (Figure 7A), SOM and TN are highly correlated with RDA1 in the negative direction and significantly positively correlated with ***norank_c_AD3***. This group is relatively enriched in the DCK group; ***Norank_f_Xanthomonaceae*** is positively correlated with pH and mainly distributed in the DPN and DEW groups; ***Bradyrhizobium*** is strongly associated with SMC; ***Norank_c_TK10*** and ***Norank_o_Slsterales*** are negatively correlated with AP and mainly clustered in the DCK group. In the fungal community (Figure 7B), ***unclassifiedd_f_Mortierellaceae*** is positively correlated with SOM and TN, ***Sagenomella*** is strongly correlated with SMC, ***Saitozyma*** and ***Solicocozyma*** are positively correlated with AP and AK, and Mortierella is positively correlated with SMC. The DCK group samples are distributed along the SOM and TN vector directions, while the DPN, DPS, and DEW groups are more driven by factors such as pH, AK, and SMC.

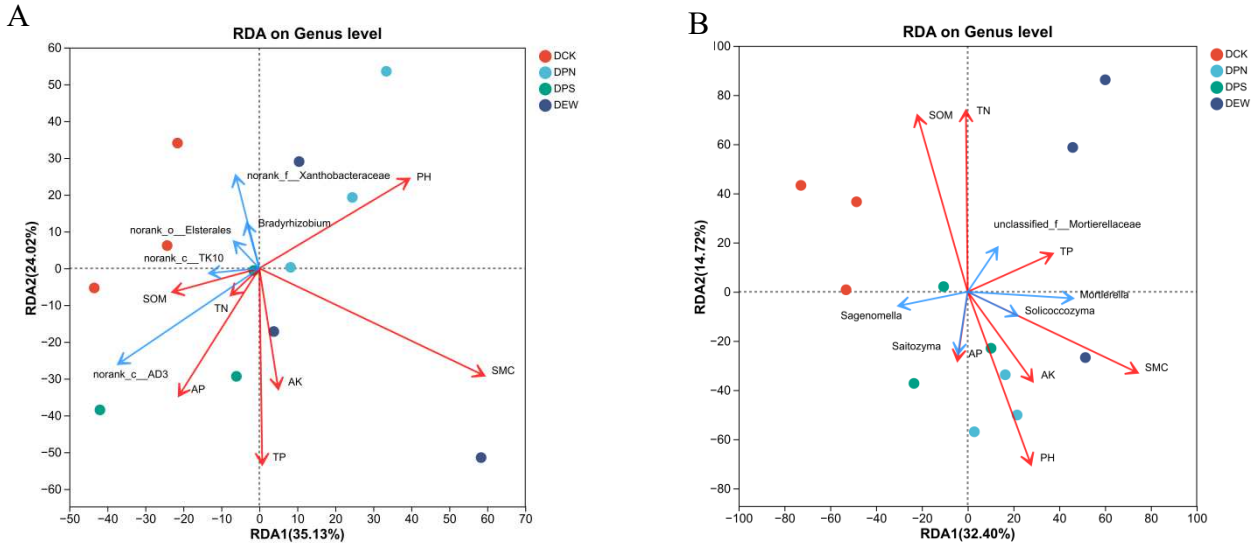


Figure 7 RDA analysis of soil physicochemical properties and microbial communities. (A) RDA results for bacterial communities. (B) RDA results for fungal communities

3.3 Mechanisms of root secretion effects on rhizosphere microbial communities in understory medicinal plants

3.3.1 Integrated consistency analysis of root secretion effects on rhizosphere microbial communities

Figure 8 evaluates the correlation between root exudates metabolome and rhizosphere microbiome data using Procrustes analysis and canonical correspondence analysis (CCA). The Procrustes analysis results showed that in the correlation analysis between bacterial community and root exudates metabolism data (Figure 8A), the M^2 value was 0.362 (P=0.001), and Dimension 1 and Dimension 2 explained 28.27% and 17.92% of the variation, respectively. The overall length of the line connecting the microbial and metabolic pairing points of each treatment group was relatively short, especially the pairing points of DCK group and DPS group were highly overlapping, indicating good consistency in the sorting structure of the two groups of data; The connection between the DEW group is relatively long, indicating weak consistency between its metabolic phenotype and bacterial community structure, and significant variation between samples. In the correlation analysis between fungal communities and metabolic data (Figure 8B), the M^2 value was 0.239 (P=0.001), and Dimension 1 and Dimension 2 explained 29.67% and 20.35% of the variation, respectively. The DCK group had the highest degree of point duplication, followed by the DPN group. The DEW group still showed significant intra group dispersion, and overall consistency was better than that of the bacterial community (M^2=0.239<0.362), indicating a higher degree of matching between root exudates and fungal community structure, and a tighter chemical biological coupling between the two.

The CCA analysis (Figure 8CD) further validated the association pattern between differential metabolites of root exudates and microbial communities at the genus level. The dominant genera and differential metabolites of bacterial (Figure 8C) and fungal (Figure 8D) communities showed a clear co distribution pattern in the sorting space, with most samples concentrated within the confidence circle. Metabolites and microbial genera showed similar distribution trends on Components 1 and 2, further supporting the hypothesis that root exudates mediate rhizosphere microbial assembly. In summary, the results of Procrustes and CCA jointly indicate a significant statistical correlation between the metabolic characteristics of root exudates in understory medicinal plants and the structure of rhizosphere microbial communities, and this correlation is stronger in fungal communities, confirming the key role of root exudates as chemical mediators in shaping the assembly of rhizosphere microbial communities. This lays the foundation for subsequent correlation network analysis of "metabolites microbial communities medicinal quality".

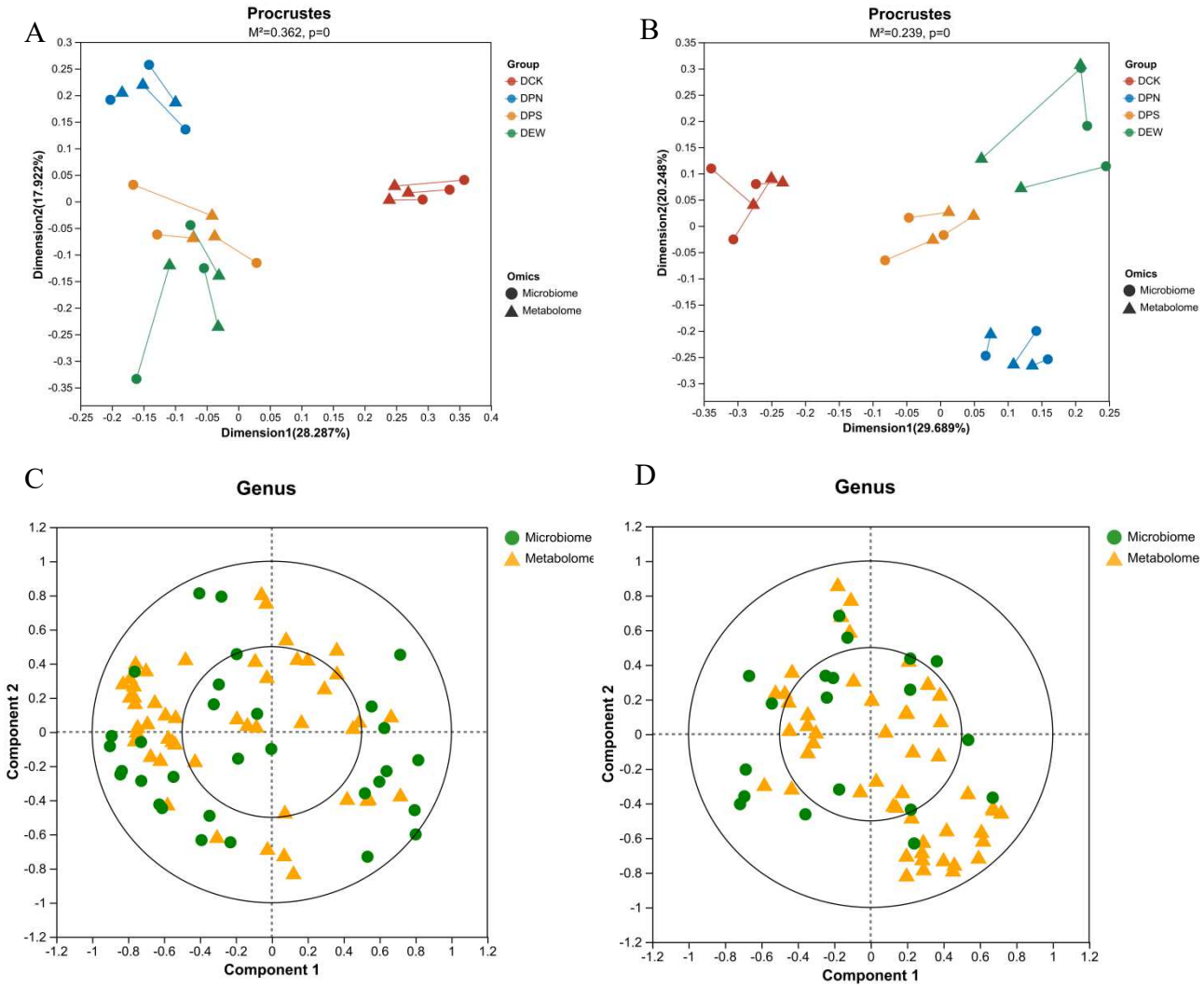


Figure 8 Procrustes and CCA analysis of root secretion effects on rhizosphere microbial communities. (A) Procrustes analysis results for bacterial communities. (B) Procrustes analysis results for fungal communities. (C) Analysis of root exudates and bacterial community CCA. (D) Analysis of root exudates and fungal community CCA.

3.3.2Association correlation analysis of root secretion on soil inter-root microbial communities

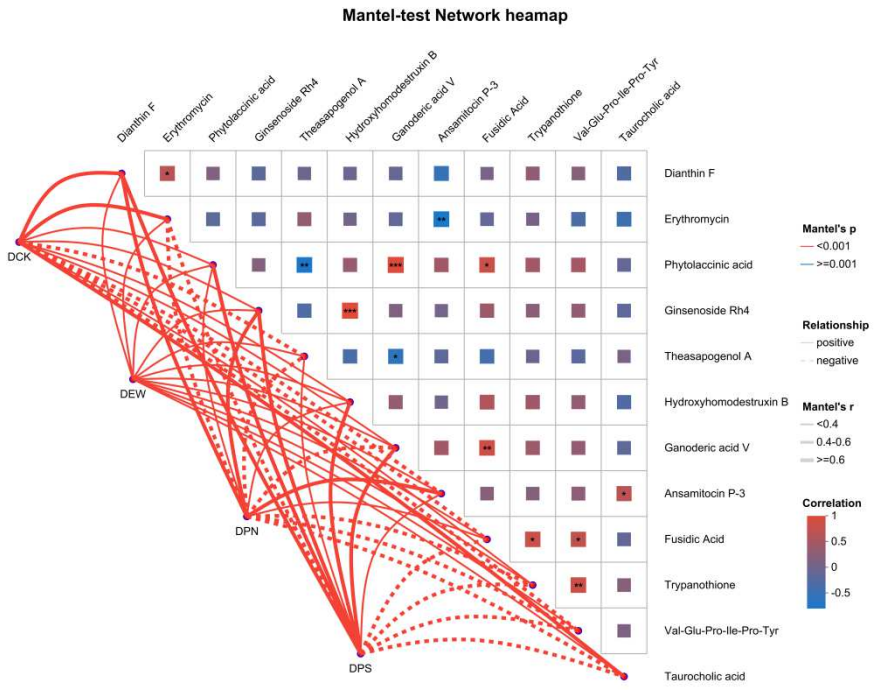
Figure 9 analyzed the correlation strength between rhizosphere soil microbial communities and key root exudates metabolites of four understory medicinal plants using Mantel test network heatmaps, revealing the coupling patterns between bacterial communities (Figure 9A) and fungal communities (Figure 9B) and differential metabolites. The Mantel test results showed that there was a significant positive correlation ($r>0.4$, $P<0.001$) between the four treatments (DCK, DPN, DPS, DEW) and most of the differential metabolites. The correlation between the red line connections was significantly greater than the negative correlation between the dashed line connections, indicating that root exudates have a positive recruitment effect on the rhizosphere microbial community as a whole.

In the bacterial community (Figure 9A), the DPN group showed a strong positive correlation with multiple metabolites ($r>0.6$, $P<0.001$, thick solid line), among which the correlation with

metabolites such as Phytolacaic acid, Ginsenoside Rh4, Fusidic Acid was the closest, indicating that the root exudates of Panax notoginseng had the strongest shaping effect on the bacterial community. This is consistent with the results of the DPN group having the highest number of differential metabolites and the most profound metabolic remodeling; The DPS group showed a negative correlation with some metabolites (such as Trypanothione, Val Glu Pro Ile Pro Tyr and other short peptide substances) (dashed line connection, r<0), indicating that certain components secreted by the root system of Polygonatum sibiricum have selective inhibitory effects on specific bacterial groups, which may be related to the allelopathic effects of alkaloid defense substances in Polygonatum sibiricum; The correlation strength between the DEW group and metabolites such as Dianthin F and Erythromycin is second (r ≈ 0.4-0.6); There is also a broad association between the DCK control group and various metabolites, but the lines are mostly dashed, and the overall correlation strength is relatively weak.

In the fungal community (Figure 9B), the DPN group also showed the strongest metabolite association, with significant positive correlations (r>0.6, P<0.001) with metabolites such as Ginsenoside Rh4 and Hydroxyhomodestruxin B; The DPS group showed a significant positive correlation with metabolites such as Trypanothione, while showing a negative correlation with some metabolites; The association between the DEW group and Val Glu Pro Ile Pro Tyr is relatively prominent. In addition, the correlation heatmap between metabolites showed that most metabolites were positively correlated with each other (red squares), among which Ginsenoside Rh4 was significantly positively correlated with Hydroxyhomodestruxin B, Fusidic Acid was significantly correlated with Trypanoshione, indicating that these metabolites may co secrete and jointly respond to changes in the rhizosphere microenvironment, forming functionally coupled metabolic modules.

A



B

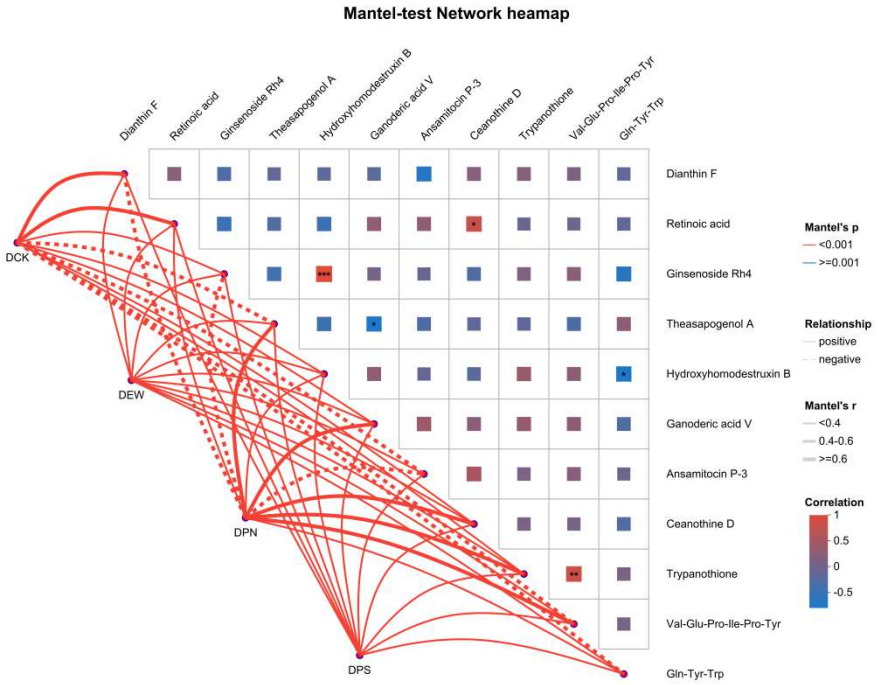


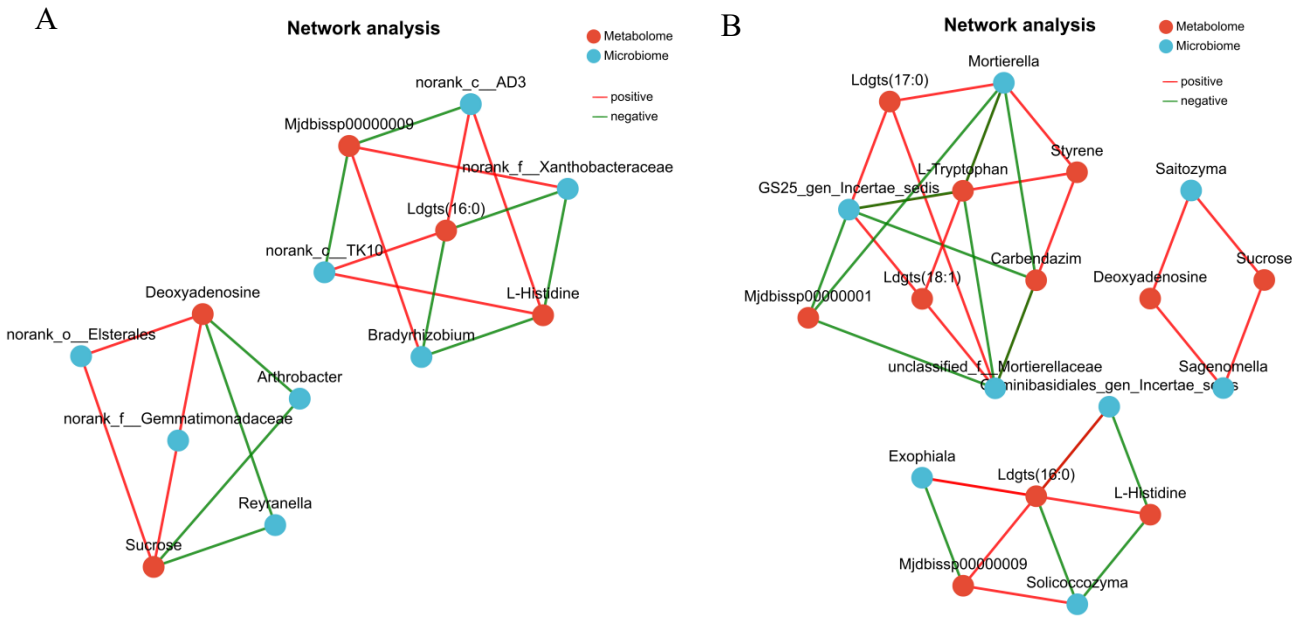
Figure 9 Mantel test analysis of root secretion effects on rhizosphere microbial communities.(A) Mantel test of root secretion effects on rhizosphere microbial communities. (B) Mantel test results for fungal communities.

Network interaction between rhizosphere microbial communities and metabolites under DPN treatment.In the bacterial community (Figure 10A), ***norank_f__Gemmatimonadaceae*** and ***norank_c__AD3*** act as the core bacterial taxa, showing strong positive correlations with lipid compounds such as Ldglts(16:0) and Ldglts(18:1) ($r > 0.6$, $P < 0.001$), while exhibiting negative correlations with nitrogen-containing metabolites such as Deoxyadenosine and L-Histidine ($r < -0.5$, $P < 0.01$), suggesting that ***Gemmatimonadaceae*** may affect plant physiology by regulating lipid metabolism. In the fungal community (Figure 10B), ***Mortierella*** and ***unclassified_f__Mortierellaceae*** are positively correlated with lipid metabolites such as Ldglts(17:0) and Mjdbissp00000009 ($r > 0.6$, $P < 0.001$), while negatively correlated with sucrose and related sugars ($r < -0.5$, $P < 0.01$); ***Saitozyma*** and ***Sagenomella*** form a complex interaction network with Sucrose and Deoxyadenosine. Network topology analysis shows that DPN treatment promotes the accumulation of beneficial lipid metabolites by reshaping microbial–metabolite associations, while inhibiting redundant carbohydrate metabolism, providing key evidence for deciphering the microbial mechanisms underlying the formation of medicinal plant quality.

Network interaction between rhizosphere microbial communities and metabolites under DPS treatment.In the bacterial community (Figure 10C), ***norank_c__TK10*** and ***Arthrobacter*** are the core bacterial groups, strongly positively correlated with lipid compounds such as Ldglts(16:0) and Mjdbissp00000009 ($r > 0.6$, $P < 0.001$), while negatively correlated with alkaloid-like metabolites such as L-Histidine and L-Tryptophan ($r < -0.5$, $P < 0.01$); norank_g__AD3 was negatively correlated with Ldglts(17:0) and Styrene, etc. ($r < -0.5$, $P < 0.01$). The fungal community (Figure 10D) shows that ***Mortierella*** and ***Saitozyma*** are positively correlated with lipid compounds such as Ldglts(17:0) and Ldglts(18:1) ($r > 0.6$, $P < 0.001$), while negatively correlated with Carbendazim and

L-Tryptophan (r<−0.5, P<0.01); ***unclassified_f__Mortierellaceae*** forms a complex interaction network with secondary metabolites such as Sucrose and Styrene. Network topology analysis shows that DPS treatment optimizes the allocation strategy of rhizosphere metabolites by regulating the microbial functional niche, providing functional evidence for elucidating the microbially driven mechanism of quality formation in medicinal plants.

Network interaction between rhizosphere microbial communities and metabolites under DEW treatment.In the bacterial community (Figure 10E), ***norank_f__Gemmatimonadaceae*** and ***norank_c__AD3***, as the core bacterial genera, showed strong positive correlations with nitrogen-containing and aromatic metabolites such as L-Histidine and Styrene (r > 0.6, P < 0.001), while with lipid compounds such as Ldglts(16:0) and Ldglts(18:1) they showed negative correlations (r<−0.5, P<0.01); ***Bradyrhizobium*** showed a negative correlation with Deoxyadenosine and Mjdbissp00000001, etc. (r<−0.5, P<0.01). The fungal community (Figure 10F) shows that ***Mortierella*** is positively correlated with lipid compounds such as Ldglts(16:0) and Mjdbissp00000009 (r>0.6, P<0.001), while negatively correlated with ***Sollicocezyma, Exophiala***, etc. (r<−0.5, P<0.01). Network topology analysis shows that DEW treatment promotes the accumulation of nitrogen-containing metabolites by reshaping the microbial–metabolite associations, while inhibiting lipid compound synthesis, forming a functional differentiation with DPN treatment, providing key evidence for elucidating the microbial mechanisms underlying the quality formation of medicinal plants under different treatments.



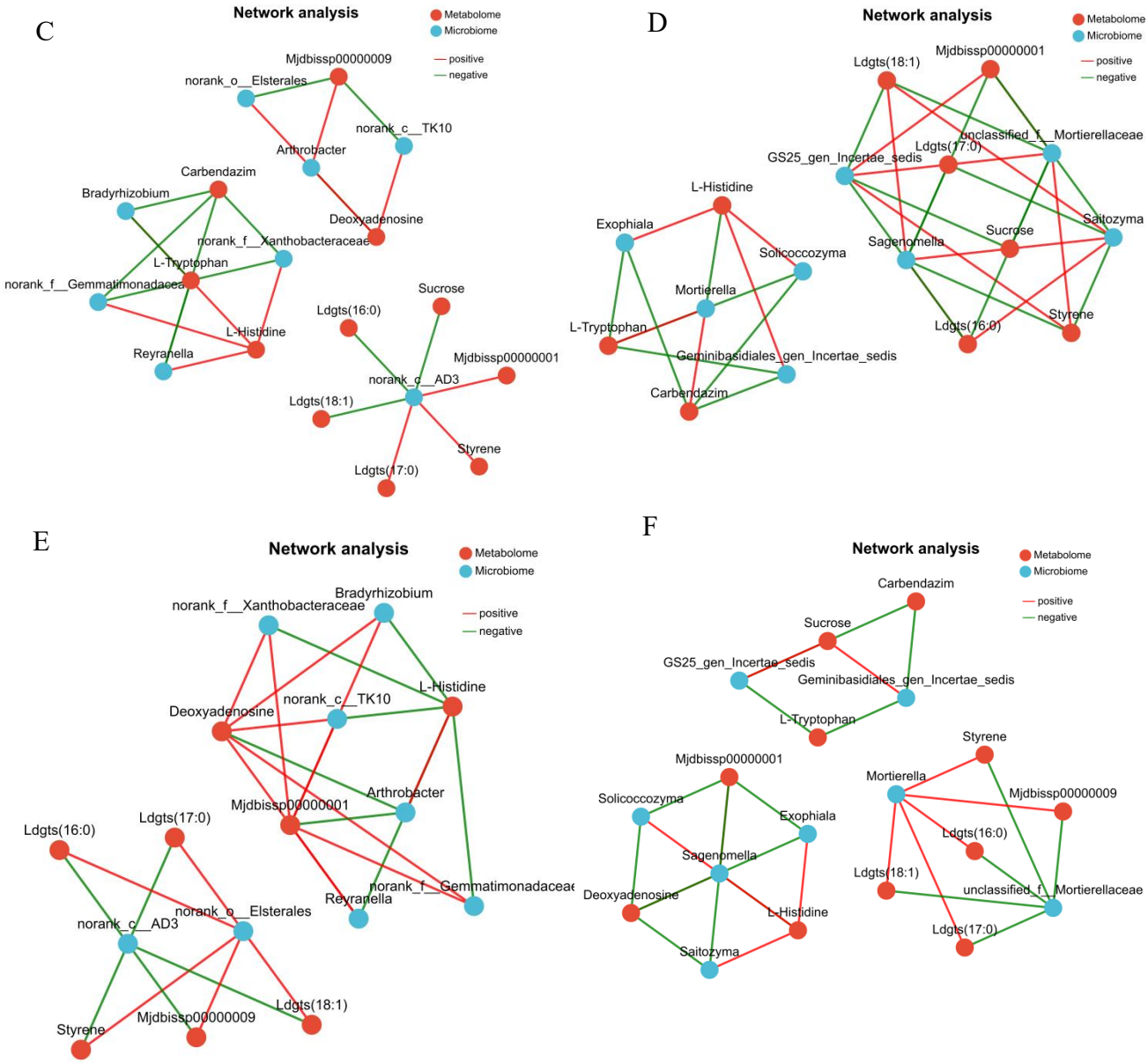


Figure 10 Analysis of the correlation network diagram between root exudates and soil rhizosphere microbial community.(A) Correlation network diagram of DPN bacterial community. (B) Correlation network diagram of DPN fine fungal community.(C) Correlation network diagram of DPS bacterial community. (D) Correlation network diagram of DPS fine fungal community.(E) Correlation network diagram of DEW bacterial community. (F) Correlation network diagram of DEW fine fungal community.

4 Discussions

The structural attributes of microbial communities represent a critical factor governing soil quality and plant health in systems where medicinal herbs are cultivated beneath forest canopies, and pronounced compositional divergence typically occurs across contrasting habitats and management regimes [21]. In the present work, both bacterial and fungal communities exhibited clear separation in structure and relative abundance between the unplanted natural forest (DCK) and the three cultivated treatments, and cultivated plots supported higher microbial diversity than the

natural stand; the under-canopy ***Panax notoginseng*** site (DPN) recorded the greatest Shannon values for both bacteria (≈4.55) and fungi (≈6.35) [22]. The chemical richness of belowground plant inputs offers a convincing explanation for this pattern. The secretions, apoplastic residues, and rhizosphere sediments released by the three herbs supplied rhizosphere microbes with plentiful carbon and energy, and their composition was dominated by lipids and lipid-like molecules, organic acids and derivatives, organic oxygen compounds, and phenylpropanoids and polyketides, with lipids constituting the single largest category [23]. Since lipids and organic acids prevailed in the metabolic responses of these plants, they plausibly widened the range of accessible substrates and thereby fostered higher microbial diversity and the coexistence of additional species [24]. In parallel, the organic acids, amino acids, and sugars contained in the exudates strongly modulate soil microbial growth and metabolism, invigorating microbial activity and thereby shaping the transformation and cycling of soil nutrients [25]. Of particular interest, the marked interspecific heterogeneity in exudate chemistry—exemplified by the elevated alkaloid share in one species and the exclusive organic sulfur compounds of the cruciferous species, which align with its glucosinolate-centered metabolism—implies that each plant deploys a species-specific chemical program in structuring its rhizosphere microbiome, and this offers a mechanistic account of why fungal communities responded more sensitively to planting treatments than bacterial ones in our data [26]. It must also be stressed that these three species are grown as perennial, no-till, continuously cropped plants; sustained high-density monocropping may permit harmful taxa to accumulate and microbial diversity to decline, raising the risk of severe soil-borne root rot [27].

Our findings additionally identified a set of potentially detrimental rhizosphere taxa—notably the bacterial genus Bradyrhizobium and fungal lineages related to Saitozyma and Sebacina—whose occurrence tracked changes in the rhizosphere community and whose proliferation may undermine the capacity of medicinal plants to resist soil-borne pathogens [28]. These taxa can weaken host resistance and heighten vulnerability to infection, thereby suppressing growth and yield; their enrichment may simultaneously reorganize the rhizosphere community and crowd out beneficial microbes, upsetting the soil's ecological equilibrium [29]. Once established on root tissues, such pathogens may provoke disorders typified by root rot, curtailing the uptake of water and nutrients and constraining whole-plant development [30]. The redundancy analysis (RDA) strengthened this interpretation by showing that soil physicochemical variables (SOM, TN, AP, AK, SMC, and pH) accounted for 59.15% and 47.12% of the cumulative variation in bacterial and fungal communities, respectively, which suggests that community turnover may feed back into nutrient transformation and cycling and, ultimately, into soil fertility and plant nutrition [31]. Pathogen-driven growth inhibition may present as stunted development and depressed yields, while broader community degradation could erode ecosystem services such as water conservation, carbon sequestration, and nitrogen fixation, with potentially adverse effects on the integrity of the entire understory ecosystem [32]. Cultivation itself may also reshape soil physicochemical conditions—pH, nutrient levels, and porosity—and thus modify microbial habitats and enzyme activities [33]. In practical terms, curbing the dominance of harmful flora appears to be a viable route to root rot control, and refining understory planting schemes—via moderated planting density, intercropping, or rotation—may raise rhizosphere microbial diversity and activity while safeguarding soil fertility[34]. Appropriate supplementation of soil nutrients and moisture may further enrich the active constituents of root secretions and improve the ecological resilience of the plants [35].

The mechanistic link between rhizosphere microbes and root exudates across the three plantations was interrogated through an integrated suite of approaches—Procrustes analysis, CCA, Mantel tests, and correlation network construction—exposing treatment-dependent configurations of microbe–metabolite association [36]. The Procrustes statistics substantiated a significant statistical concordance between exudate chemistry and microbial architecture, with the tighter coupling detected for fungi[37]. Under ***Panax notoginseng*** treatment, the pivotal bacterial taxa ***norank_f__Gemmatimonadaceae*** and ***norank_c__AD3*** displayed robust positive associations with lipid compounds including Ldglts(16:0) and Ldglts(18:1) ($r > 0.6$, $P < 0.001$), whereas the fungal taxa ***Mortierella*** and ***unclassified_f__Mortierellaceae*** correlated positively with lipid metabolites such as Ldglts(17:0) and negatively with sucrose and cognate sugars—evidence that this treatment favors the build-up of advantageous lipid metabolites while restraining superfluous carbohydrate turnover[38]. Under ***Polygonatum sibiricum*** treatment, the central bacterial groups ***norank_c__TK10*** and ***Arthrobacter*** associated positively with lipid compounds yet negatively with nitrogen-bearing metabolites such as L-Histidine and L-Tryptophan, and the fungal taxa ***Mortierella*** and ***Saitozyma*** correlated positively with lipids but negatively with carbendazim and L-Tryptophan, pointing to a realignment of microbial functional niches and a re-prioritization of metabolite allocation within the rhizosphere [39]. The ***Eutrema wasabia*** treatment followed the reverse configuration: its core bacterial taxa allied positively with nitrogen-containing and aromatic metabolites including L-Histidine and styrene while turning against lipids, even as ***Mortierella*** retained positive ties to lipid compounds, thereby establishing a functional divergence from the ***Panax notoginseng*** regime [40]. Considered collectively, the three treatments reorganized the microbial–metabolite network and steered the accumulation of lipids, nitrogen-containing metabolites, and sugars along distinct trajectories, furnishing compelling evidence for the microbially mediated processes that underpin quality formation in medicinal plants [41].

In conclusion, the root exudates of understory medicinal herbs function as chemical mediators that selectively orchestrate the assembly of rhizosphere bacterial and fungal assemblages, and each planting pattern generates a characteristic "variety–microbiota–metabolite" interaction network with far-reaching ecological implications[42]. Prospective research should prioritize the fine-scale identification of exudate constituents, longitudinal surveillance of microbial communities across developmental stages and seasons, and the joint appraisal of environmental drivers, thereby underpinning the sustainable cultivation of Chinese medicinal materials [43]. Such efforts will not only guide the refinement of understory planting designs and the enhancement of herb quality, but will also provide a foundation for the long-term prosperity of the understory forest economy [44].

5 Conclusions

(1) The chemical characteristics of root exudates exhibit significant species specificity: ***Panax notoginseng***, ***Eutrema wasabia***, and ***Polygonatum sibiricum*** secreted 355, 241, and 236 significantly different metabolites compared with the non-planted control (DCK), respectively, with 89 identical differential metabolites shared among the three species. HMDB classification analysis showed that lipids and lipid-like molecules accounted for the largest proportion in all three species, followed by organic acids and their derivatives, organic oxygen compounds, and phenylpropanoids and polyketides, reflecting the differences in plant ecological functions, pharmacological effects, and rhizosphere adaptation strategies.

(2) The composition and diversity of microbial communities are regulated by root exudates:

the structure, abundance, and diversity of dominant bacterial phyla (***Pseudomonadota, Acidobacteriota, Chloroflexita, Actinomycota***) and fungal phyla (***Ascomycota, Basidiomycota, Mortierellomycota***) were significantly shaped by exudate inputs. Procrustes analysis confirmed that exudate metabolites were significantly coupled with microbial community structure , and the Mantel test revealed significant positive correlations ($r>0.4$, $P<0.001$) between planting treatments and most differential metabolites, indicating that root exudates exert a positive recruitment effect on rhizosphere microorganisms, with fungal communities showing a tighter chemical–biological coupling.

(3) Enrichment of metabolic pathways reveals differential adaptation strategies: ***Panax notoginseng*** enriched 71 pathways (23 significant), with plant hormone signal transduction, aminoacyl tRNA biosynthesis, and TCA cycle as the core, to enhance nitrogen metabolism and defensive secondary metabolism; ***Polygonatum sibiricum*** 52 (16 significant), highlighting nucleotide metabolism and ABC transporters, with a focus on substance transport; 44 (8 significant) ***Eutrema wasabia*** are characterized by linoleic acid metabolism and flavonoid biosynthesis. Plant hormone signal transduction is a common pathway that reflects differentiation adaptation under the interaction of "variety-environment-metabolism".

(4) The microbial–metabolite interaction network exhibits treatment specificity: in the DPN treatment, ***norank_f__Gemmatimonadaceae*** and ***norank_c__AD3*** (bacteria) were strongly positively correlated with lipid compounds such as Ldglts(16:0) and Ldglts(18:1) ($r > 0.6$, $P < 0.001$), while ***Mortierella*** and ***unclassified_f__Mortierellaceae*** (fungi) were positively correlated with lipid metabolites and negatively correlated with sucrose; in the DPS treatment, ***norank_c__TK10*** and ***Arthrobacter*** (bacteria) were positively correlated with lipids, and ***Mortierella*** and ***Saitozyma*** (fungi) were positively correlated with lipid compounds but negatively correlated with Carbendazim and L-Tryptophan; in the DEW treatment, the core bacterial taxa were positively correlated with nitrogen-containing and aromatic metabolites such as L-Histidine and Styrene but negatively correlated with lipids, while ***Mortierella*** remained positively correlated with lipid compounds. The three treatments regulate the accumulation of different metabolites by reshaping the microbial–metabolite association network.

(5) Ecological significance and applications: Through nutrient inputs and chemical-signal mediation, root exudates shape rhizosphere microbial assemblages, favoring beneficial microbial taxa and stimulating their metabolic functions. Our findings unravel the microbe-driven mechanisms governing quality development in medicinal plants, highlight the importance of plant-microbe interplay for ecosystem regulation, and draw attention to pathogen build-up associated with continuous monocropping. This work provides theoretical support for refining understory cultivation regimes, sustaining soil fertility, and advancing eco-friendly forest-understory economic systems.

Data availability statement

The raw data supporting the conclusions of this article will be made available by the authors, without undue reservation.

https://doi.org/10.57760/sciencedb.26666

https://doi.org/10.57760/sciencedb.26303

Author Information

1. College of Agriculture and Biotechnology, Yunnan Agricultural University, Kunming, Yunnan 650500, China
2. School of Soil and Water Conservation, Southwest Forestry University, Kunming, Yunnan 650224, China

Yuan YANG[1], Jianqiang LI[2]*, Bo YANG[2], Wen CHEN[2], Wenqi TANG[2], Lianling CHA[2]

Author contributions

Y.Y. was the first author, responsible for the overall design and conceptualization of the study, writing the first draft of the paper, and reviewing and revising the final manuscript.J.Q.L. was the corresponding author, responsible for data collection and analysis, participating in the discussion of the paper, and checking the data of the paper.B.Y. was responsible for the design and implementation of the experimental part, assisted in data collection, and interpreted the experimental results.W.C. was responsible for writing the literature review, participating in the paper discussion, and embellishing the language of the paper.W.Q.T. was responsible for the research methodology and modeling, participated in data analysis and interpretation, and wrote the methodology section of the paper.L.L.C. was responsible for the preparation of research materials and maintenance of experimental equipment, assisting in the implementation of the experiment, and recording the experimental process.All authors critically reviewed the manuscript, and agreed to the final version.

Funding

Youth Talent Special Project of Yunnan Province's "Xingdian Talent Support Program" (XDYC-QNRC-2022-0205); Kunming Science and Technology "Announcement and Leadership System" Project (2021-J-H-002-02); First Class Discipline of Soil and Water Conservation and Desertification Control in Yunnan Province (SBK20250001)

Acknowledgments

The author thanks the School of Soil and Water Conservation at Southwest Forestry University for its financial support and technical assistance.

Conflict of interest

The authors declare that the research was conducted in the absence of any commercial orfinancial relationships that could be construed as a potential conflict of interest.

Publisher's note

All claims expressed in this article are solely those of the authors and do not necessarilyrepresent those of their affliated organizations, or those of the publisher, the editors and thereviewers. Any product that may be evaluated in this article, or claim that may be made by itsmanufacturer, is not guaranteed or endorsed by the publisher.

Ethics, Consent to Participate, and Consent to Publish declarations: not applicable.

References

[1]Xiang Y P, Xiao F. Development strategies for under-forest Chinese medicinal materials industry in Yunnan Province[J]. Forest Inventory and Planning, 2022, 47(02): 166-171.

[2]Feng Z H, Tian X, Wang L, et al. Suitable under-forest planting area selection for five typical Chinese me dicinal materials in Yunnan integrating climate data and stand conditions[J]. Journal of Southwest Forestry University, 2025, 45(03): 112-121.

[3]Yang M, Luo L F, Zhu S S. Research progress on root exudates of Panax notoginseng alleviating continuo us cropping obstacles by regulating rhizosphere beneficial microorganisms under autotoxic stress[J]. Journal of Yunnan Agricultural University (Natural Science), 2023, 38(02): 189-198.

[4]Meng Z C, Tian Q, Zhi J Z, et al. Prediction of potential suitable areas of Polygonatum kingianum in Chi na based on Maxent model[J]. Journal of Tropical and Subtropical Botany, 2025, 33(06): 821-830.

[5]Zhang Y, Li Y, Guo T. Research progress on release pathways and regulatory mechanisms of plant root ex udates[J]. Chinese Journal of Soil Science, 2021, 52(03): 735-742.

[6]Yin X T, Li G, Wang P. Mediating effects of root exudates on underground inter-specific interactions in cr op diversity systems[J]. Chinese Journal of Eco-Agriculture, 2022, 30(08): 1261-1272.

[7]Wang F, Liu H, Li T. Research progress on autotoxicity and regulation of continuous cropping obstacles in medicinal plants[J]. China Journal of Chinese Materia Medica, 2024, 49(05): 1201-1210.

[8]Zhou Y F, Li C Y, Yang M. Research progress on the mechanism of root exudates-mediated intercropping for prevention and control of soil-borne diseases[J]. Journal of Yunnan Agricultural University (Natural Sc ience), 2022, 37(06): 981-990.

[9]Chang Y F, Yu W H, Chen H P, et al. Effects of planting years on rhizosphere soil microbial activity and function of healthy Panax notoginseng[J]. Soils, 2023, 55(01): 112-120.

[10] Ge X M, Wang K C, Zhang C L. Fungal diversity in rhizosphere soil of healthy and root-rot diseased P olygonatum cyrtonema under different cultivation patterns[J]. Chinese Agricultural Science Bulletin, 2024, 40(12): 108-116.

[11]Li L, Wang X, Zhang H W. Research progress on bidirectional interaction mechanism between root exudat es and rhizosphere environment[J]. Chinese Journal of Ecology, 2020, 39(11): 3829-3838.

[12]Sun J, Liu M, Zhang Y M. Root exudates: hub for material and information exchange among plant-soil-m icrobe[J]. Acta Pedologica Sinica, 2023, 60(02): 345-358.

[13]Liu W W, Yao L G, Wang J. Root-exudates-driven evolution of soil physicochemical properties and micro bial community[J]. Ecological Science, 2022, 41(03): 1-9.

[14]Yuan Y, He X H, Zhu S S. Effects of rhizosphere microbial community succession on soil enzyme activit ies under continuous cropping of Panax notoginseng[J]. Journal of Yunnan Agricultural University (Natural Science), 2024, 39(01): 97-105.

[15]Zhu S S, Yang M, Luo L F. Ecological mechanisms of continuous cropping obstacles induced by autotoxi

c substances in medicinal plants[J]. Plant Physiology Journal, 2021, 57(07): 1425-1438.

[16]Li S J, Huang L Q. Advances in medicinal plant rhizosphere microbiome and soil-health regulation[J]. Act a Microbiologica Sinica, 2025, 65(04): 1321-1338.

[17]Liu Y, He X H, Huang H C. Relationship between rhizosphere microbial community imbalance and root-r ot disease of medicinal plants[J]. Plant Protection, 2023, 49(02): 1-10.

[18]Qian Y, Wang Q, Yang W Q. Research gaps and prospects of interaction between root exudates and rhizo sphere microorganisms of under-forest medicinal plants[J]. World Forestry Research, 2025, 38(02): 28-34.

[19]Zhang C P, Chen S, Wang Y. Rhizosphere microecology and sustainable cultivation of medicinal plants un der agroforestry systems[J]. Scientia Agricultura Sinica, 2022, 55(18): 3635-3648.

[20]He X H, Yang M, Zhu S S. Approaches for soil-health management in ecologically cultivated Chinese me dicinal materials[J]. Chinese Journal of Soil Science, 2021, 52(06): 1485-1494.

[21]Li H, Zhang J S, Meng P. Research progress on driving mechanism of rhizosphere microbial community i n forest-medicinal plant complex system[J]. Acta Ecologica Sinica, 2022, 42(18): 7297-7308.

[22]Li J H, Li J Q, Gao L, et al. Cultivation of Panax notoginseng in forestland alters the soil microbial co mmunity[J]. Microbiology China, 2024, 51(6): 1995-2012.

[23]Dai Y, Yang Q, Niu L L, et al. Effects of root exudates on soil microorganisms under compound medicin al-plant planting modes[J]. Chinese Journal of Applied Ecology, 2024, 35(3): 789-798.

[24]Zhou X, Liu Y, Shi S. Carbon substrate utilization of rhizosphere microorganisms responding to root-exuda te components of perennial medicinal herbs[J]. Soils, 2023, 55(4): 761-769.

[25]Chen Y, Liu Z, Wang H. Amino-acid and organic-acid components in root exudates regulating rhizosphere nutrient cycling of forest-grown medicinal plants[J]. Chinese Journal of Soil Science, 2024, 55(1): 112-12 1.

[26]Wang Q, Lin Y, Chen L. Differential responses of bacteria and fungi to root-exudate chemical spectra of multiple medicinal herbs[J]. Acta Microbiologica Sinica, 2023, 63(8): 3124-3138.

[27]Sun K, Liu B, Zhang C. Research progress on continuous-cropping obstacles of medicinal plants: soil degr adation and rhizosphere microecological imbalance[J]. Journal of Forestry Research, 2025, 36(2): 411-424.

[28]Wang H J, Guan H L, Wang Y, et al. Comparative analysis of rhizosphere microbial community characteri stics of root-rot diseased Panax notoginseng under natural forest and field conditions[J]. Microbiology Chi na, 2023, 50(5): 1988-2001.

[29]Hu Y, Gao Y, Zheng Y. Rhizosphere microbial community disorder induced by enrichment of opportunistic pathogenic taxa in continuously-cultivated medicinal herbs[J]. Plant Physiology Journal, 2025, 61(3): 581-594.

[30]Zhang B, He X H, Yuan Y. Physiological damage and nutrient-absorption disorder induced by root-rot pat hogens in Panax notoginseng[J]. Journal of Yunnan Agricultural University (Natural Science), 2023, 38(4): 672-680.

[31]Wu Y, Meng Q X, Zhao J. Driving effects of soil physicochemical properties on rhizosphere microbial co mmunities of forest-cultivated Chinese medicinal materials[J]. Ecological Science, 2022, 41(5): 45-54.

[32]Xu L, Zhang J, Li M. Ecosystem-service decline induced by rhizosphere microbiome degradation in medic inal-plant agroforestry[J]. Chinese Journal of Eco-Agriculture, 2024, 32(4): 612-624.

[33]Yang S J. Responses of soil physicochemical-properties and enzyme activities to forest-understory medicina l-plant cultivation[J]. Journal of Northeast Forestry University, 2024, 52(3): 89-96.

[34]Huang Y G, Xiong B J, Shi R. Regulatory effects of intercropping and rotation modes on rhizosphere mic ro-ecology of under-forest Panax notoginseng[J]. Journal of South China Agricultural University, 2025, 46 (2): 210-218.

[35]Zhang A, Li B, He S. Regulation effects of soil water-nutrient supply on root-exudate profiles and plant e cological resilience of under-forest medicinal herbs[J]. Chinese Agricultural Science Bulletin, 2025, 41(8): 98-106.

[36]Luo H, Qian Y, Wang Q. Application of mantel-test, procrustes and network analysis in rhizosphere micro be-metabolite interaction research of medicinal plants[J]. World Forestry Research, 2024, 37(1): 36-44.

[37]Zhao K, Mo S, Yang W Q. Procrustes-based matching between root-exudate metabolome and rhizosphere microbiome under agroforestry medicinal-plant cultivation[J]. Acta Pedologica Sinica, 2023, 60(5): 1422-14 35.

[38]Zhong S J, Deng L M, Luo L F, et al. Lipid metabolites in rhizosphere regulating key beneficial bacterial and fungal groups of Panax notoginseng[J]. Chinese Journal of Plant Ecology, 2024, 48(7): 821-833.

[39]Ge X M, Wang K C, Sun T. Microbial-metabolite correlation characteristics in rhizosphere of Polygonatum cyrtonema under forest cultivation[J]. Plant Physiology Journal, 2023, 59(10): 1945-1958.

[40]Zeng Y, Liu S, He J. Differences of rhizosphere microbial-metabolite networks between cruciferous medici nal herbs and perennial rhizome medicinal plants[J]. Acta Botanica Boreali-Occidentalia Sinica, 2024, 44 (2): 289-302.

[41]Jiang L, Zheng H, Kong D. Microbially mediated formation of medicinal quality under different rhizospher e microbe-metabolite network patterns[J]. China Journal of Chinese Materia Medica, 2025, 50(7): 1891-19 04.

[42]Wang R, Li Y. “Variety-microbiota-metabolite” interactive network in rhizosphere of agroforestry-cultivate d medicinal plants[J]. Chinese Journal of Ecology, 2022, 41(8): 1587-1596.

[43]Qian Y, Wang Q, Yang W Q. Current challenges and research priorities for rhizosphere ecology of forest-grown medicinal plants[J]. Journal of Plant Resources and Environment, 2023, 32(3): 1-10.

[44]Xie T, Deng L M, Mei X Y. Optimization directions for under-forest medicinal-plant planting system base d on rhizosphere micro-ecological theory[J]. Forest Inventory and Planning, 2024, 49(2): 134-142.

Supplementary Files

This is a list of supplementary files associated with this preprint. Click to download.

- Imagedata.zip
- KEGGPERMISSION26290434811.pdf